Study of instability driven mixing via improved tracking and transport control

Xiaolin Li, Wurigen Bo, James Glimm and the FronTier Team

Department of Applied Math and Statistics

SUNY at Stony Brook

Outline of the talk

1. PDE, conservation law, and discontinuity
2. Improving the front tracking method
3. Comparison and benchmarks
4. Comparison of Rayleigh-Taylor instability
5. Transport control with tracking
6. Conclusion
7. Application to other scientific and engineering problems

PDE

- Hyperbolic equation (wave equation)
- Parabolic equation (diffusion equation)
- Elliptic equation (steady state equation)

Parabolic equations

In 1-D: $\dfrac{\partial u}{\partial t} = D\dfrac{\partial^2 u}{\partial x^2}$ or $u_t = Du_{xx}$

In multi-dimension: $u_t = D\Delta u$

where $\Delta = \sum_{i=1}^{d} \dfrac{\partial^2}{\partial x_i^2}$ is the Laplace operator

Parabolic equation flattens all variation (variation deminishing.

Physically, it is the diffusion equation originated from the heat transfer equation.

Solution in infinite space

Initial condition: $u(x,0) = \varphi(x)$

Solution in infinite domain $(-\infty, \infty)$

$$u(x,t) = \frac{1}{\sqrt{4\pi Dt}} \int_{-\infty}^{\infty} e^{-\frac{(x-y)^2}{4Dt}} \varphi(y)dy$$

1. Singularity: $\varphi(x) = \delta(x)$

2. Discontinuity: $\varphi(x) = h(x)$

Singular initial condition

$$\varphi(x) = \delta(x) = \begin{cases} \infty & x = 0 \\ 0 & x \neq 0 \end{cases}$$

$$u(x,t) = \frac{1}{\sqrt{4\pi Dt}} e^{-\frac{x^2}{4Dt}}$$

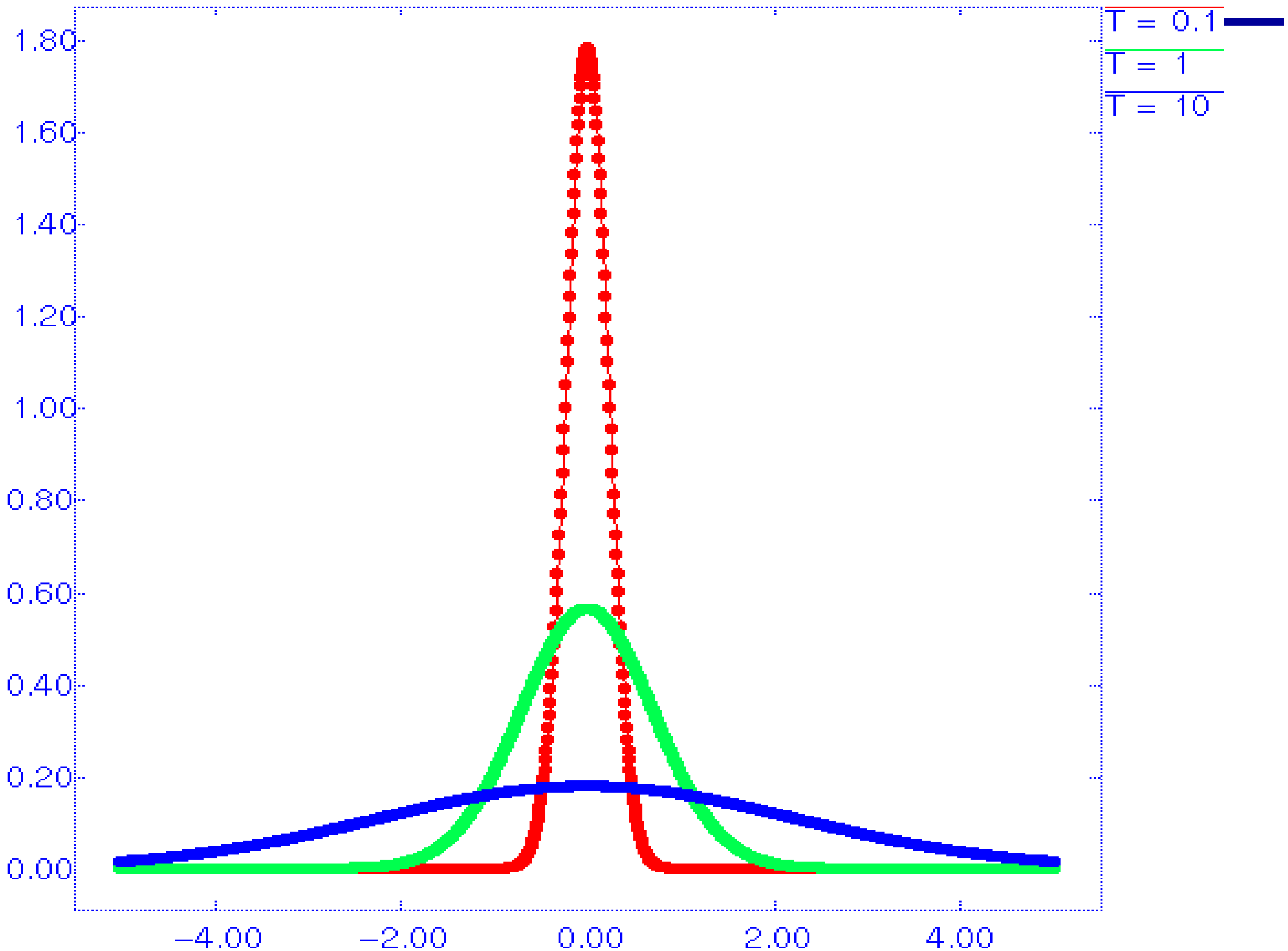
1.80
1.60
1.40
1.20
1.00
0.80
0.60
0.40
0.20
0.00
−4.00
−2.00
0.00
2.00
4.00
T = 0.1
T = 1
T = 10

Discontinuous initial condition

$$\varphi(x) = h(x) = \begin{cases} 1 & x \le 0 \\ 0 & x > 0 \end{cases}$$

$$u(x,t) = 1 - \frac{1}{\sqrt{\pi}} \int_{-\infty}^{\frac{x}{\sqrt{4Dt}}} e^{-y^2}\, dy$$

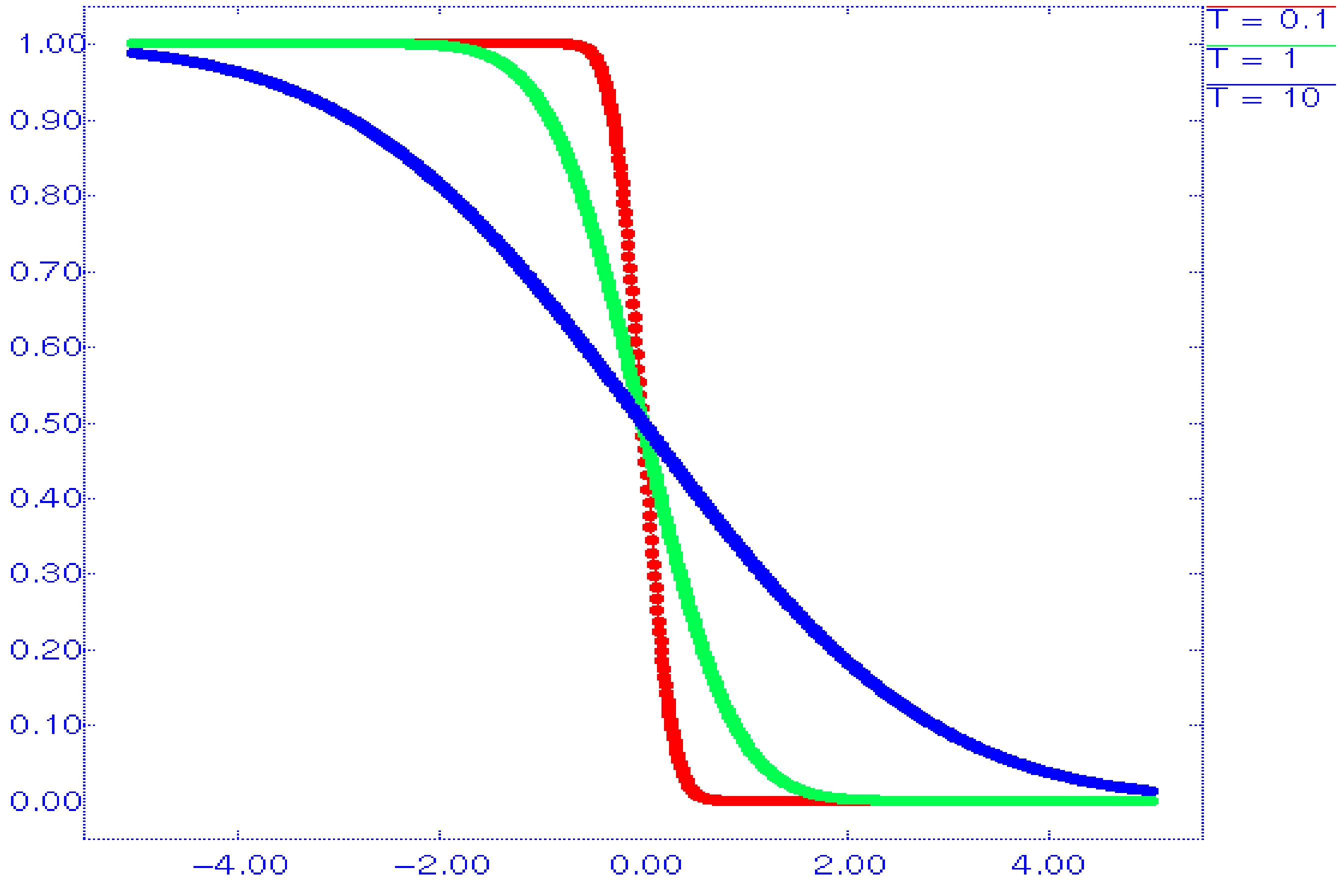

T = 0.1
T = 1
T = 10
1.00
0.90
0.80
0.70
0.60
0.50
0.40
0.30
0.20
0.10
0.00
−4.00
−2.00
0.00
2.00
4.00

Hyperbolic equation

1-D wave equation:

$$u_{tt} - a^2 u_{xx} = 0 \quad \Rightarrow \quad u_t + a u_x = 0 \quad u_t - a u_x = 0$$

Traveling wave solution:

$$u(x,t) = \varphi(x - at) \quad u(x,t) = \psi(x + at)$$

Characteristics, along the curve

$$\frac{dx}{dt} = a, \quad \frac{du}{dt} = 0$$

Linear and nonlinear equations

Linear equation: $a = a(x,t)$

Typical equation: $u_t + au_x = 0 \quad a = const$

Nonlinear equation: $a = a(x,t,u)$

Typical equation (Burgers equation)

$$u_t + uu_x = 0, \quad a = u$$

Conservation law:

$$u_t + f(u)_x = 0, \quad a = f'(u)$$

Shock Wave

1. Shock is a result of the intersection of characteristics.
2. Shock is a discontinuity across which physics change sharply.
3. Shock speed is derived from conservation—Rankine-Hugoniot condition

$$s[u] = [f(u)]$$

$$[u] = u_R - u_L \quad [f(u)] = f(u_R) - f(u_L)$$

s is the shock speed.

Examples of conservation law

1. Traffic Flow in a highway
2. Flood wave
3. Glaciers motion
4. Chemical exchange process
5. Oil reservoir
6. Gas dynamics

Traffic flow

$$\rho_t + Q(\rho)_x = 0$$

Greenberg (1959) studied the traffic of Lincoln Tunnel and found:

$$Q(\rho) = a\rho \log \frac{\rho_j}{\rho}$$

$$a = 17.2(mph), \quad \rho_j = 228(vpm)$$

Traffic relaxation:

$$\rho - \rho_0 \propto \sqrt{\frac{1}{t}}$$

Flood wave

$$\frac{\partial A}{\partial t} + \frac{\partial Q}{\partial t} = 0$$

A: The cross sectional area of the river bed

Q: Water flux in volume

Kleitz (1858) and Seddon (1900) used balance
Between gravitational force and friction force derived:

$$Q = vA = \sqrt{\frac{A^3 g \sin\alpha}{PC_f}} \propto A^{3/2}$$

Equation for gas dynamics

Mass, momemtum and energy conservation:

$$\rho_t + (\rho u)_x = 0$$

$$(\rho u)_t + (\rho u^2 + P)_x = 0$$

$$e_t + (u(e+P))_x = 0$$

Equation of state (EOS):

$$P = P(\rho, e)$$

Riemann problem

1. Initial Condition:

$$U(x,0) = \begin{cases} U_L & x < 0 \\ U_R & x > 0 \end{cases}$$

$$U_L = \begin{pmatrix} \rho_L \\ u_L \\ p_L \end{pmatrix} \quad U_R = \begin{pmatrix} \rho_R \\ u_R \\ p_R \end{pmatrix}$$

2. Invariance of solution: $U(x,t) = V\left(\frac{x}{t}\right)$

3. Four states: $U_L, \quad U_L^*, \quad U_R^*, \quad U_R$

4. Three waves: left wave, contact, right wave.

Glimm **Scheme**

Given states at the *n*th time step: U_j^n
Glimm's scheme advances the state via:

$$U_{j+1/2}^{n+1/2} = V\left(\frac{\xi}{t^{n+1/2}}\right), \quad \xi = (j+1/2)h + \vartheta h$$

$$U_j^{n+1} = V\left(\frac{\varsigma}{t^{n+1}}\right), \qquad \varsigma = jh + \vartheta h$$

ϑ is a random variable in $\left[-\frac{1}{2}, \frac{1}{2}\right]$

The convergence of Glimm scheme is through large Number theorem and is the first significant convergence Proof for the gas dynamics equations.

Godunov scheme

$$\frac{U_j^{n+1} - U_j^n}{\Delta t} + \frac{f_{j+1/2} - f_{j-1/2}}{\Delta x} = 0$$

$$f_{j+1/2} = f\left(V\left(x_{j+1/2} / t_{n+1/2}\right)\right)$$

The Discrete Representation of The Front Tracking

Volume filling rectangular mesh (Eulerian Coord.)

(N-1) dimensional Lagrangian mesh (interface)

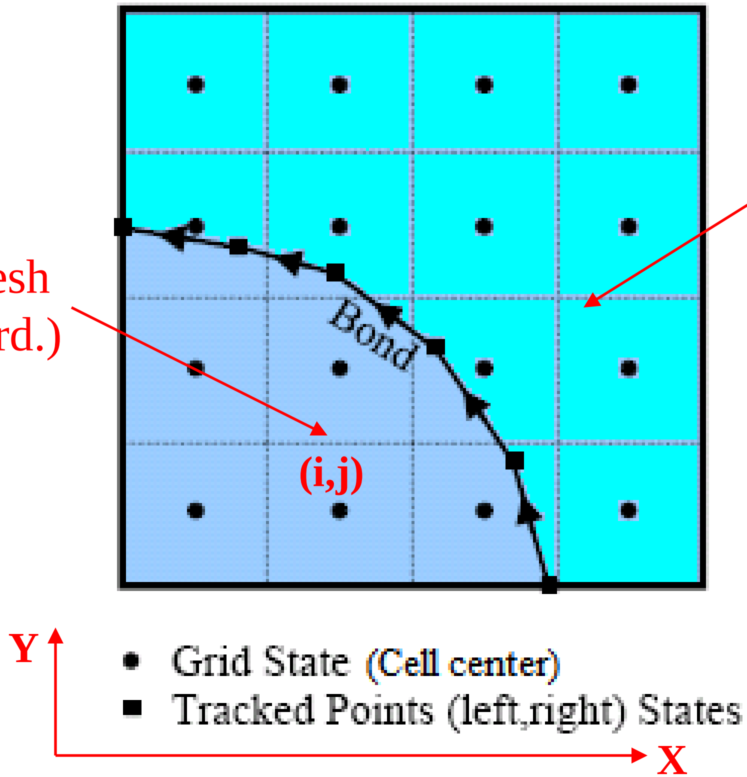

A 2D Representation

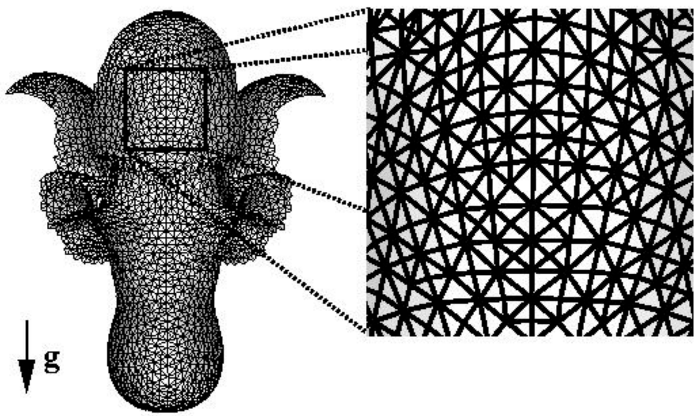

A 3D Interface

The 3D interface

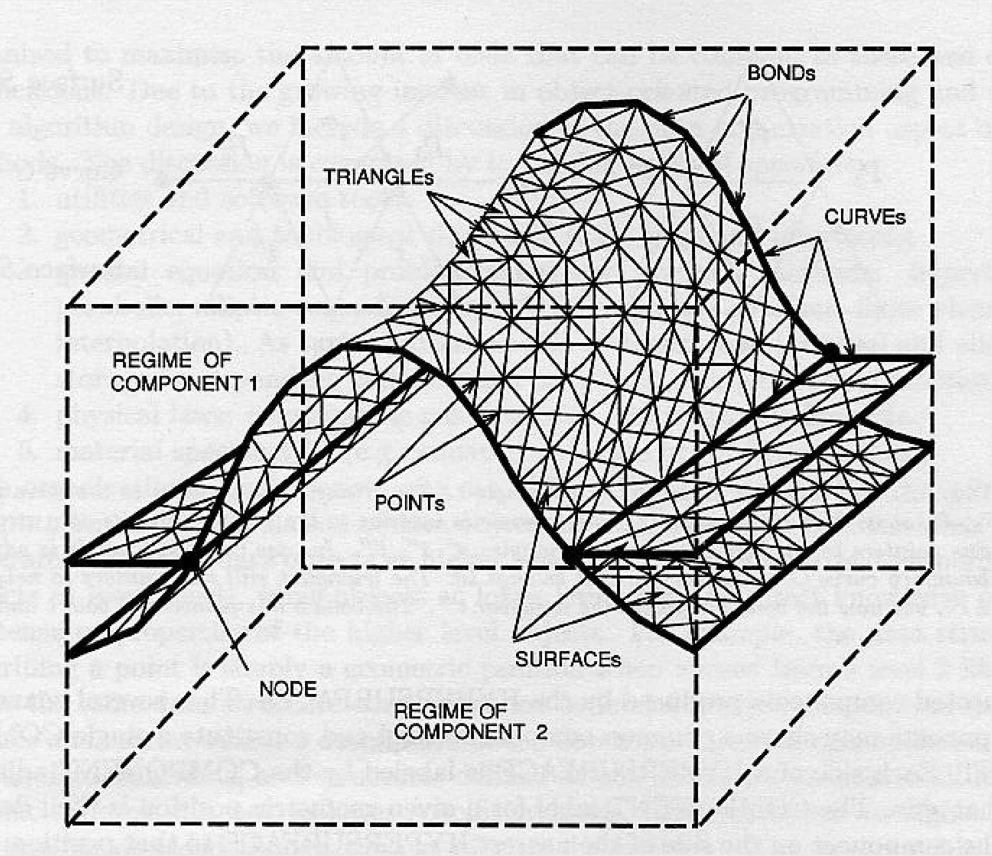

“Three Dimensional Front Tracking”,J. Glimm, J. Grove, X. L. Li, K. Shyue, Y. Zeng and Q. Zhang, SIAM J. Sci. Comp., 19, 1998.

Front Tracking Method

- Front tracking method is implemented in code *FronTier.*

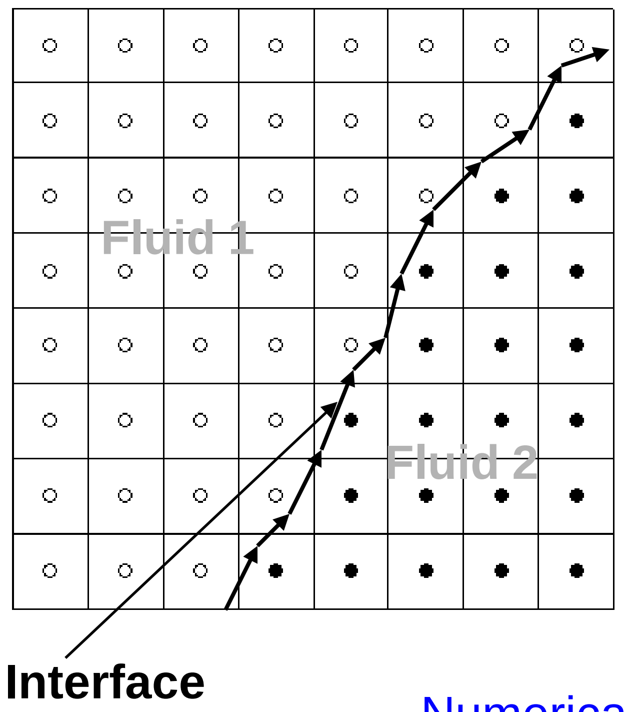

Major components:

1. A moving mesh to represent interface
2. Navier-Stokes equations
3. Dynamic subgrid scale models

Procedure to solve:

1. Propagate points on interface
2. Redistribute surface mesh
3. Reconstruct the tangled part in surface mesh
4. Solve equations for liquid and gas separately with ghost fluid method

Numerical methods related to front tracking:

1. Coupling fluid solver with interface propagation
2. Handling topological changes

Ghost Fluid Method

- The ghost states on the other side of the interface is constructed by a ghost fluid method (B.Khoo *et.al.* 2005).

- Stencil across the interface
- Solving a Riemann problem
- Using the middle states from the Riemann problem to construct the ghost states

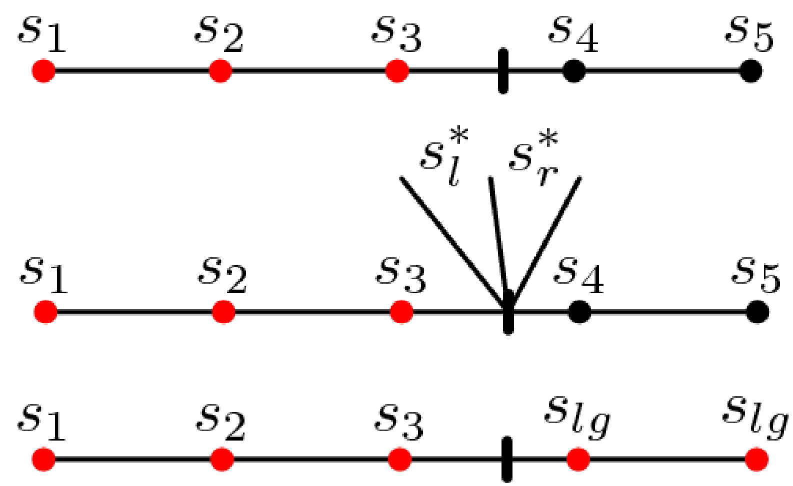

$$s_3 = (\rho_l, u_l, p_l) \quad s_l^* = (\rho_l^*, u_l^*, p_l^*)$$

$$s_{lg} = (\rho_l, u_l^*, p_l^*)$$

- Surface tension force is modeled in the Riemann problem by

$$p_l^* - p_r^* = \sigma \kappa$$

- 2D and 3D
  - Project interface normal vectors onto cell centers.
  - Construct ghost states along normal directions.

Interface Point Propagation

- Interface states are reconstructed from the interpolation of real and ghost states

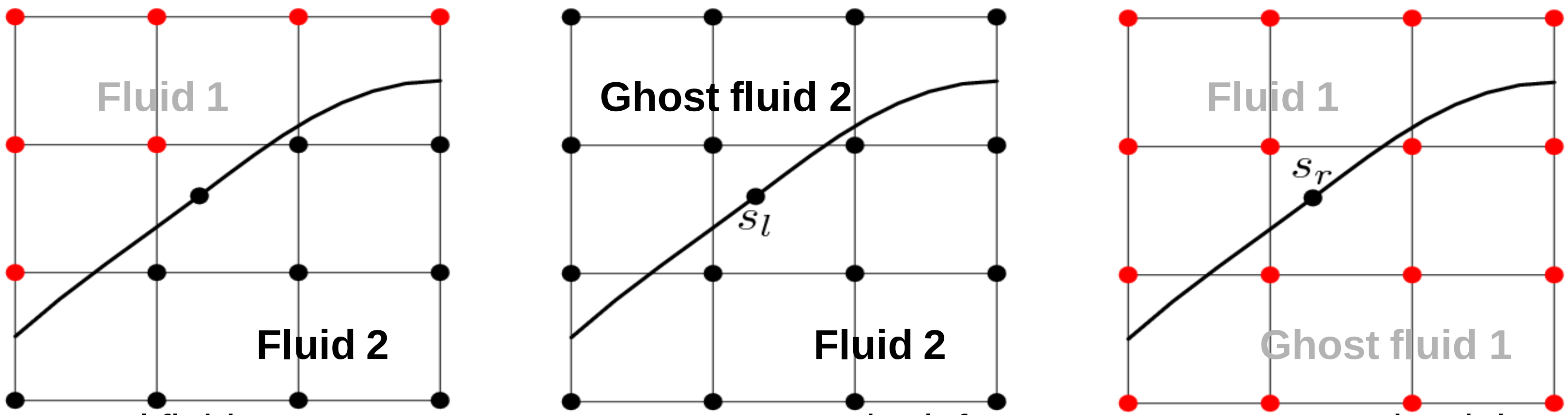

Real fluid states | Reconstruct the left interface state | Reconstruct the right interface state

Propagate interface point: $$\frac{d\mathbf{x}}{dt} = \mathbf{v}_n$$

A Riemann problem with s_l, s_r as its data is solved to determine the interface point speed $\mathbf{v}_n$

Advantage: No need to solve Navier-Stokes equations on the interface. More robust and efficient than our previous front tracking method.

Geometry and Topology

- The challenge to Lagrangian method
- Eulerian level set method
- The Marching cube method
- Reverse engineering: grid-based tracking
- Combining the best of Lagrange and Euler
- The locally grid-based tracking method

Level Set Methods

- A popular and powerful scheme for interface tracking is to compute the interface position by propagating a function whose level set corresponds to the interface position
  - The interface location at time t is given by $\phi(\mathbf{x}, t) = 0$ where

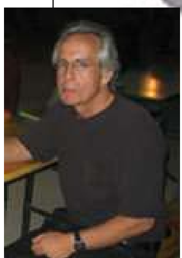

$$\phi_t + F\,|\nabla\phi| = 0$$

  - Commonly used for material interfaces
  - See the books of Sethian: “Level Set Methods and Fast Marching Methods” or Osher and Fedkiw: “Level set methods and dynamic implicit surfaces”
- Designed to handle interface topology changes automatically
  - However interface are limited to shapes that can be represented by level sets
- Couples to a numerical scheme for updating flows states on a volume mesh via a ghost fluid (extrapolation across interfaces) method
- When fully developed has similar features to explicit interface methods in many aspects

The idea of grid-based untangling

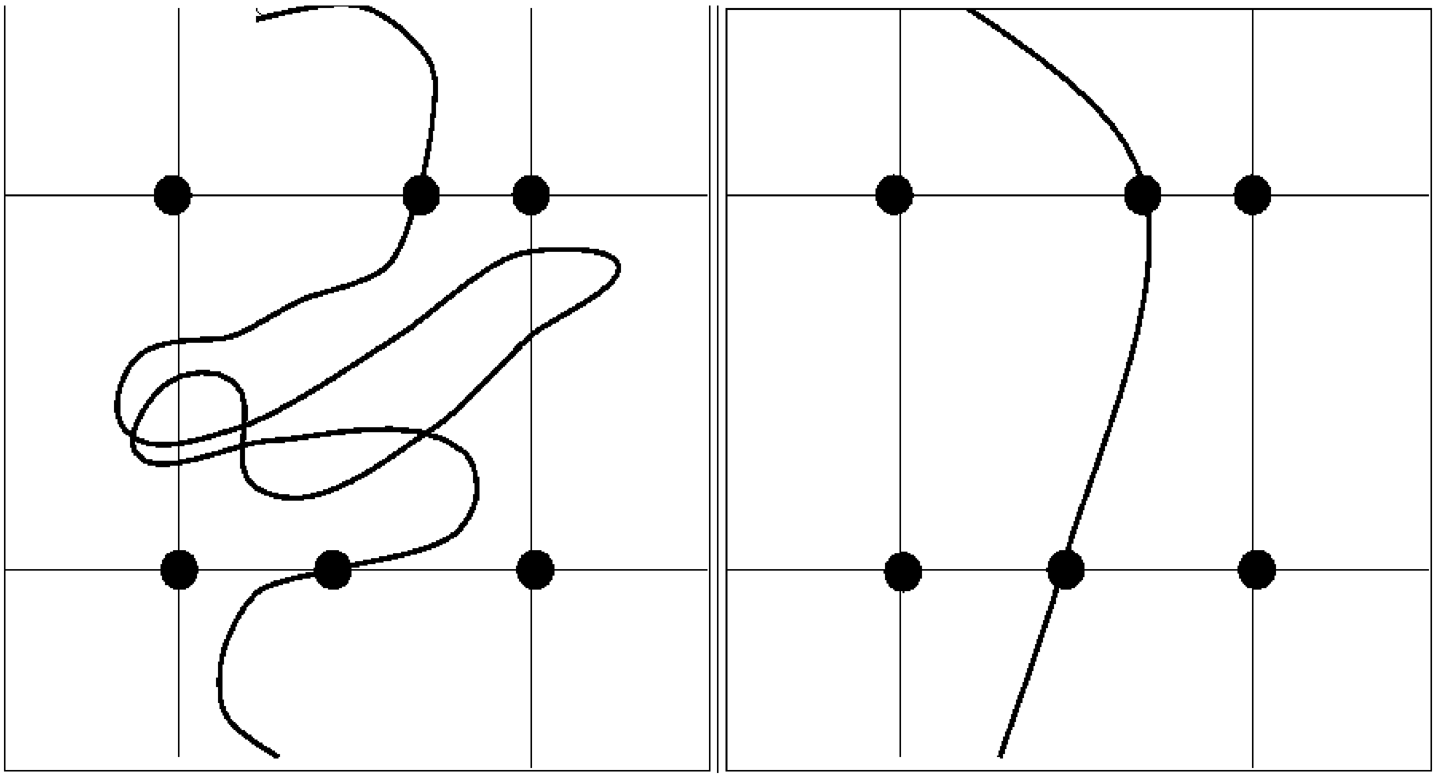

Grid-based Front Tracking

1. The common agreement: interface is greatly simplified in Eulerian grid.
2. Marching Cubes, Lorenson and Cline, 1987,

   (Static, Computer Graphics).
3. Level set method, Osher and Sethian, 1988, (Implicit).
4. Grid-based front tracking, SJSC, 21, 6 2000,

   (Explicit and Dynamic).

The 14 isomorphically distinct cases

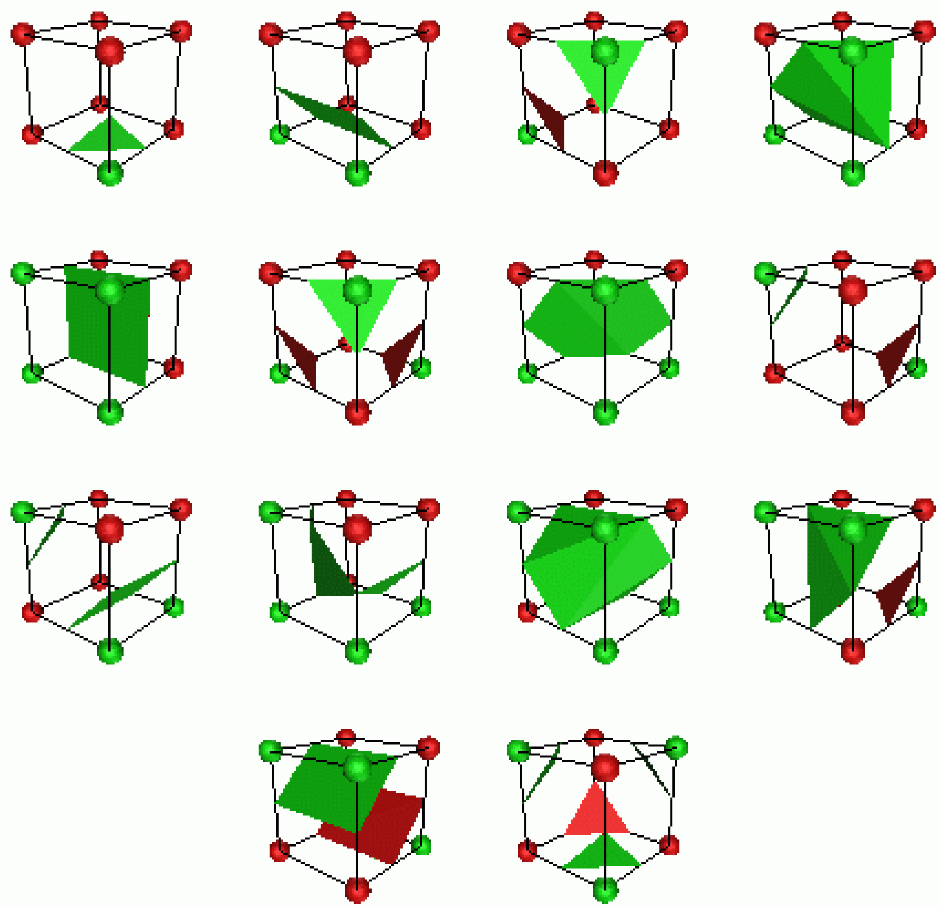

SciDAC
Scientific Discovery through Advanced Computing

Grid-based topological correction

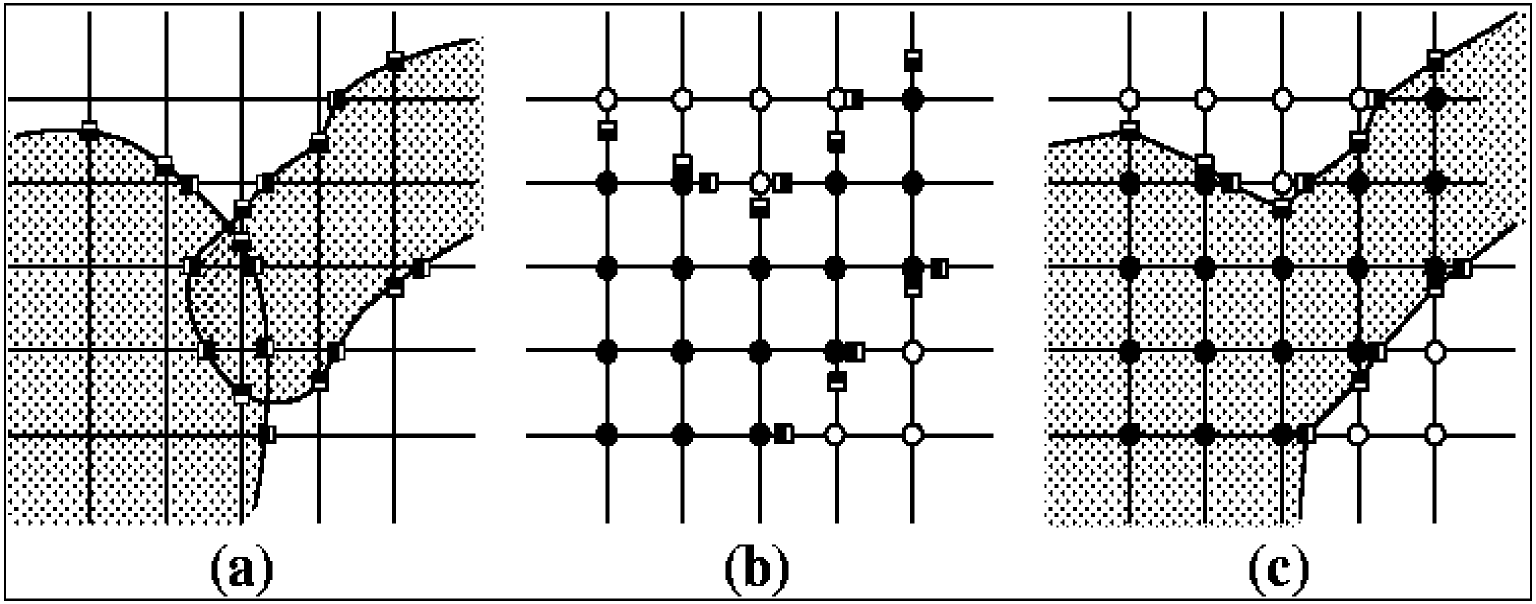

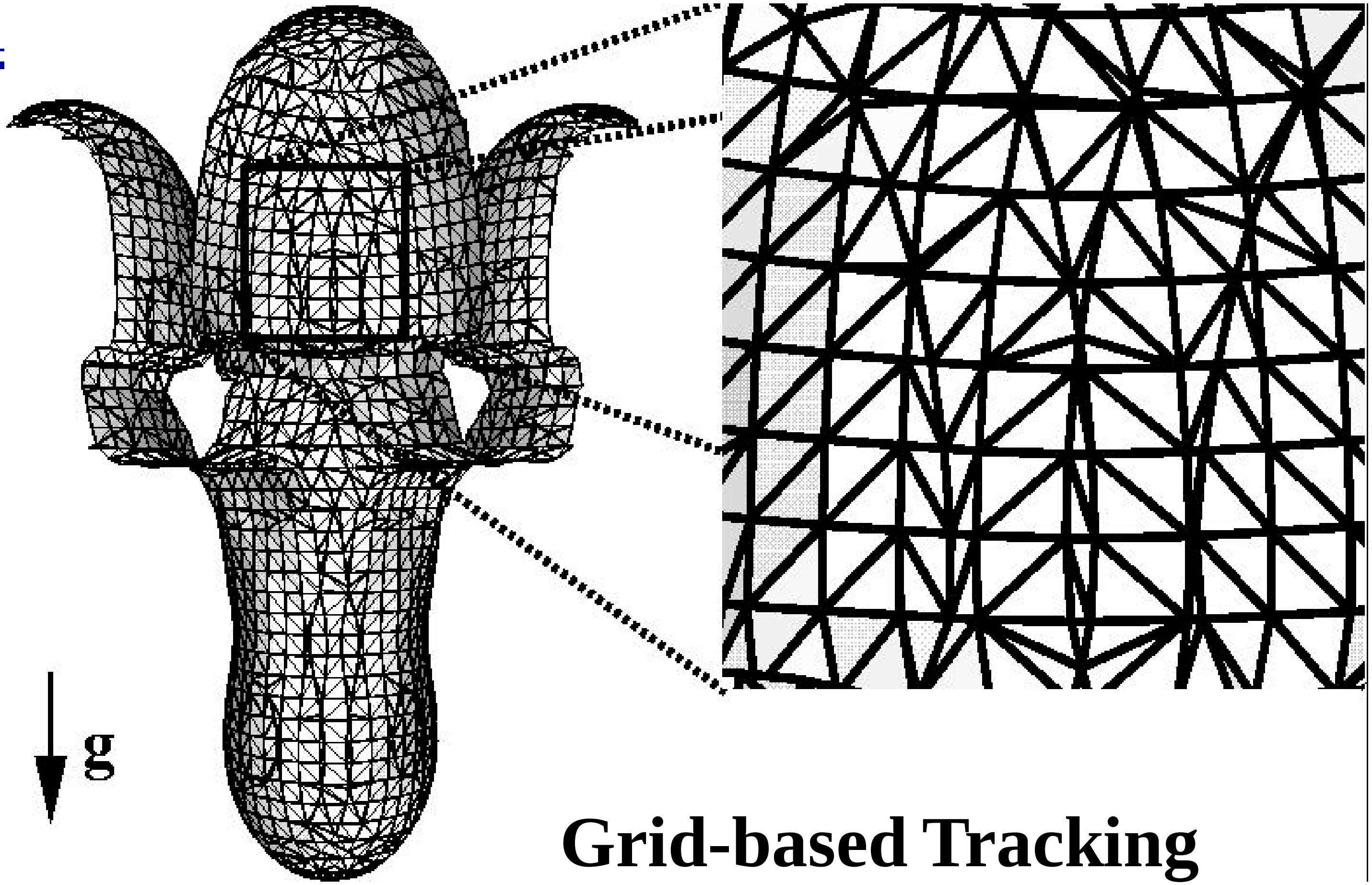

Grid-based Tracking

Interface bifurcation under grid-based front tracking method

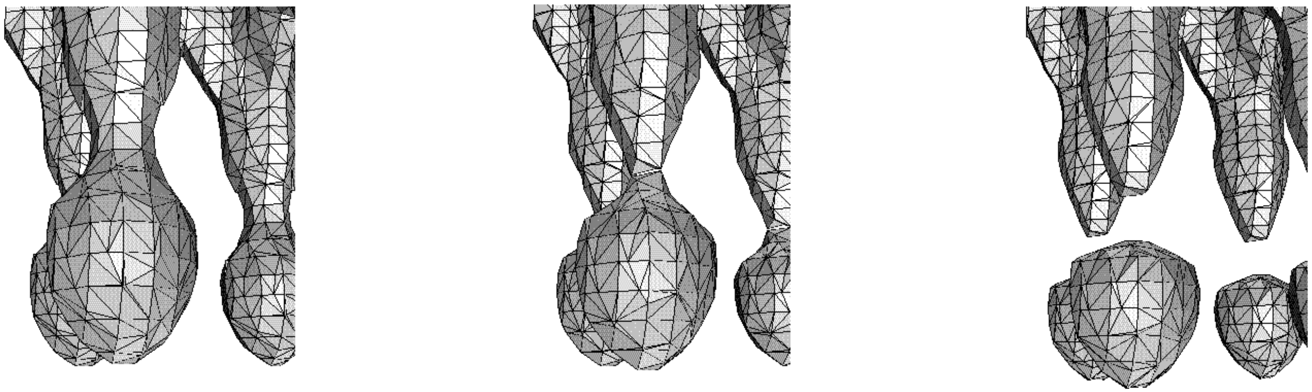

“Robust Computational Algorithm for Dynamic Interface Tracking in Three dimensions”, J. Glimm, J. Grove, X. L. Li and D. C. Tan, SIAM J. Sci. Comp., 21, 2000.

Basic FronTier Test Simulations

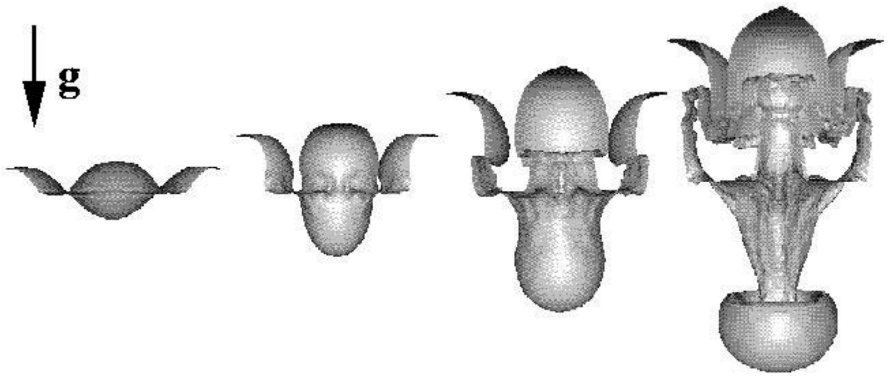

Case Single-2

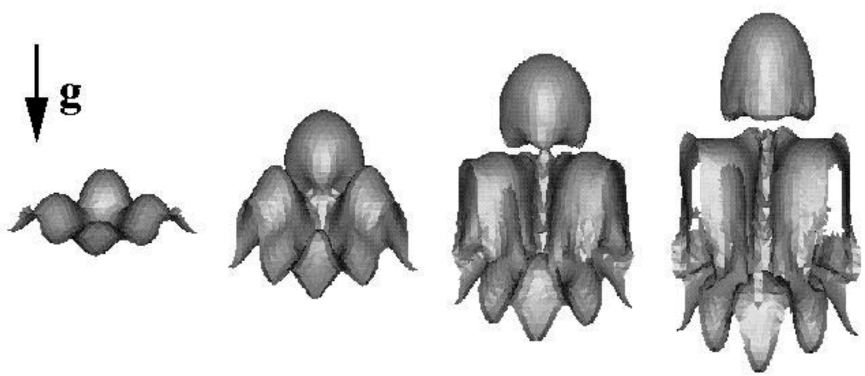

Case Bifure-1

Interface Topological Changes

- Grid based tracking is robust but too diffusive.
- Challenge: Robustness of the algorithm is crucial for large scale computing.

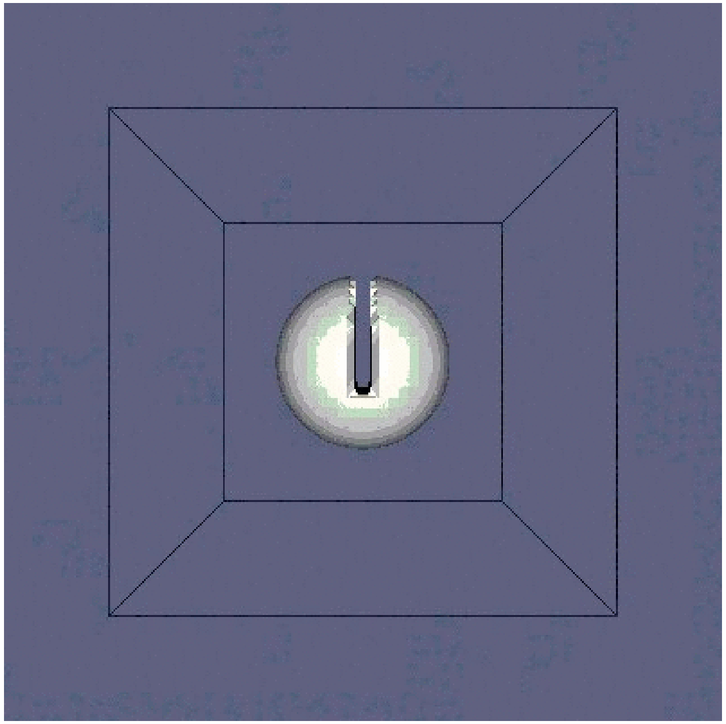

Grid based tracking

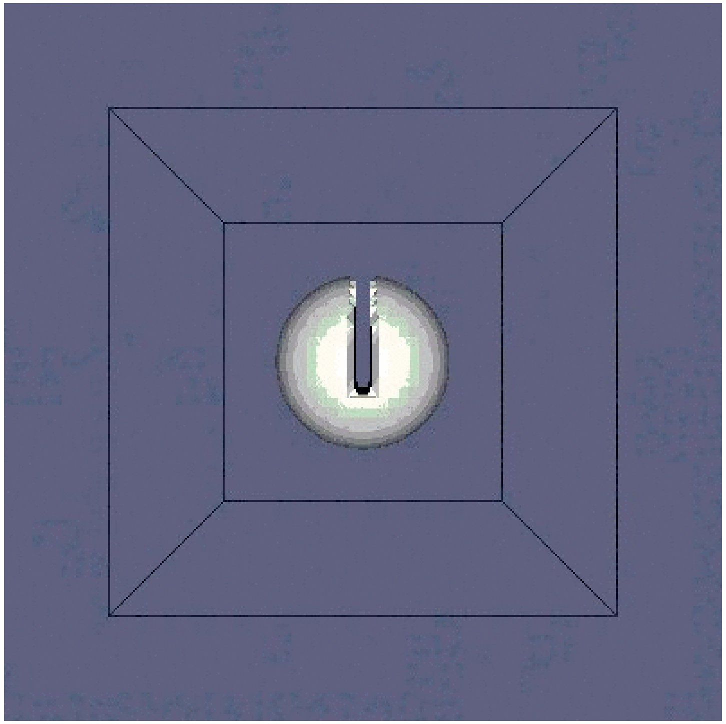

Grid free tracking

Interface Topological Changes

- Algorithms to handle topological changes
  - Grid free tracking (GF)
  - Grid based tracking (GB)
  - Locally grid based tracking (LGB)

Tangled interface

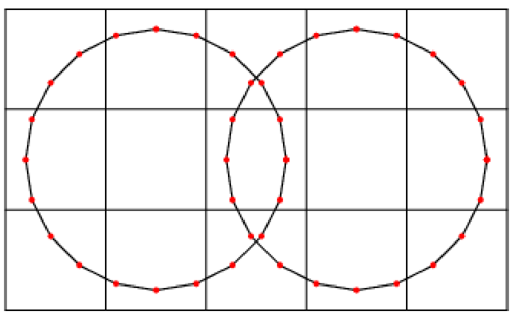

GF

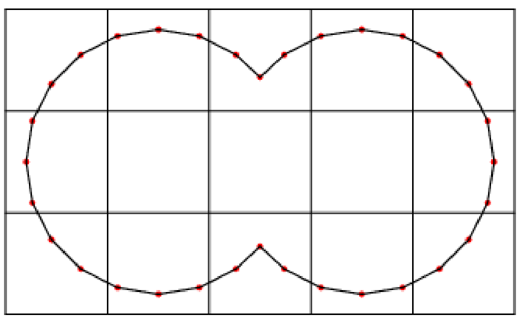

GB

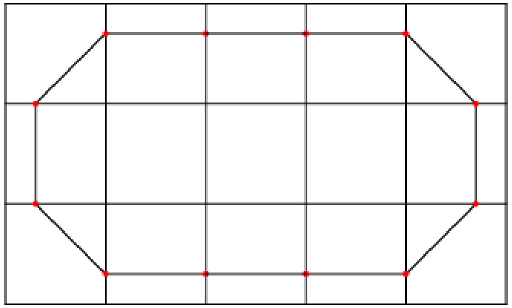

LGB

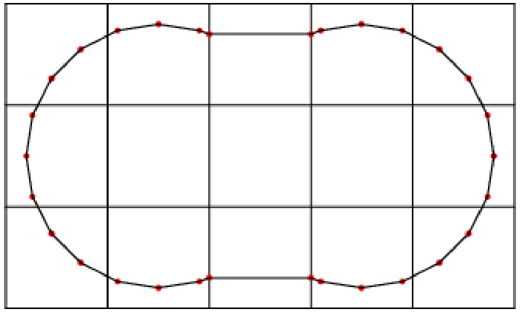

Robust Locally Grid Based (LGB) Untangle

- A robust algorithm to reconnect a grid based surface mesh with a grid free surface mesh

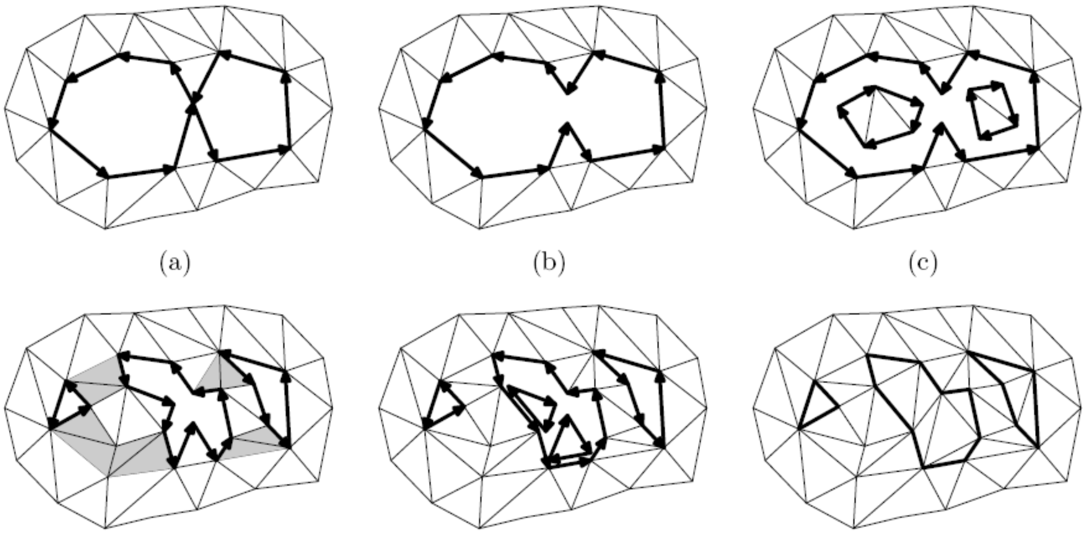

(a) (b) (c)

(d) (e) (f)

- Advantage
  - Local, it is suitable for large scale computing.
  - Robust, It generates topologically valid surface mesh.

“A Simple Package for Front Tracking”, J. Du, B. Fix, J. Glimm. X. L. Li, Y. Li, L. Wu, JCP, 213, 2006.

Benchmark Plus

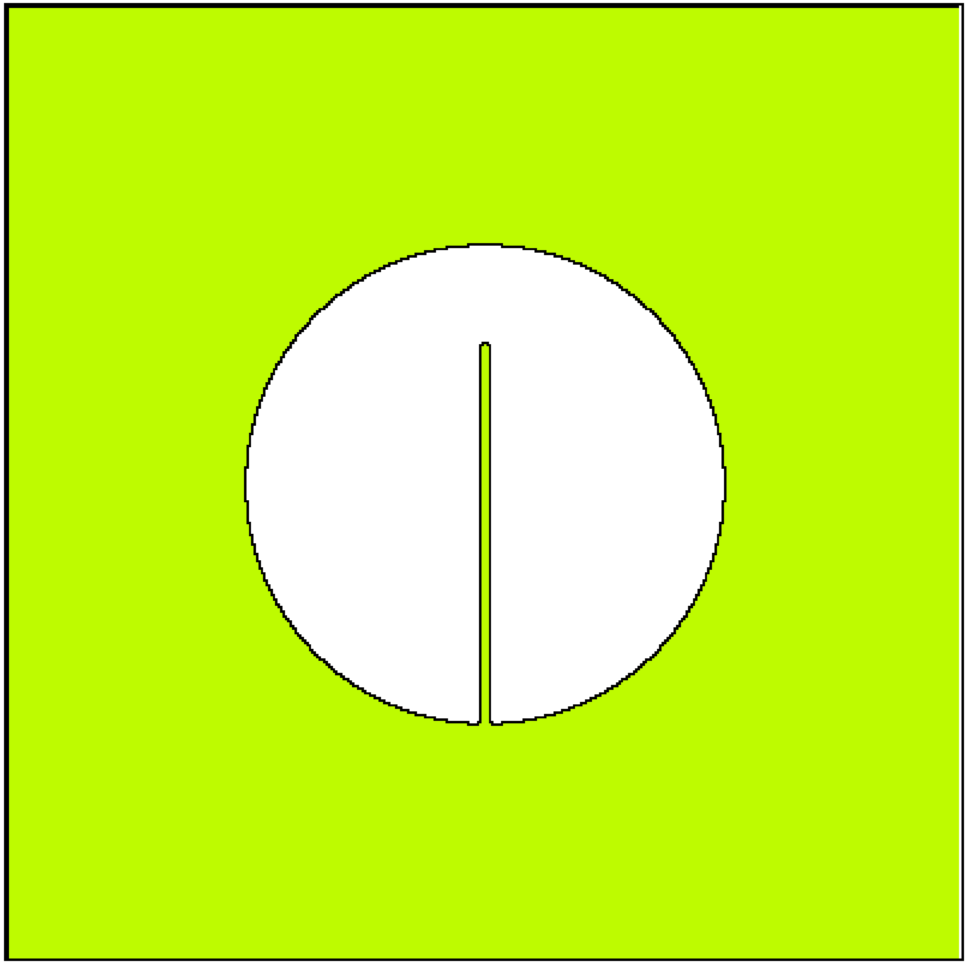

3D rotation of slotted sphere

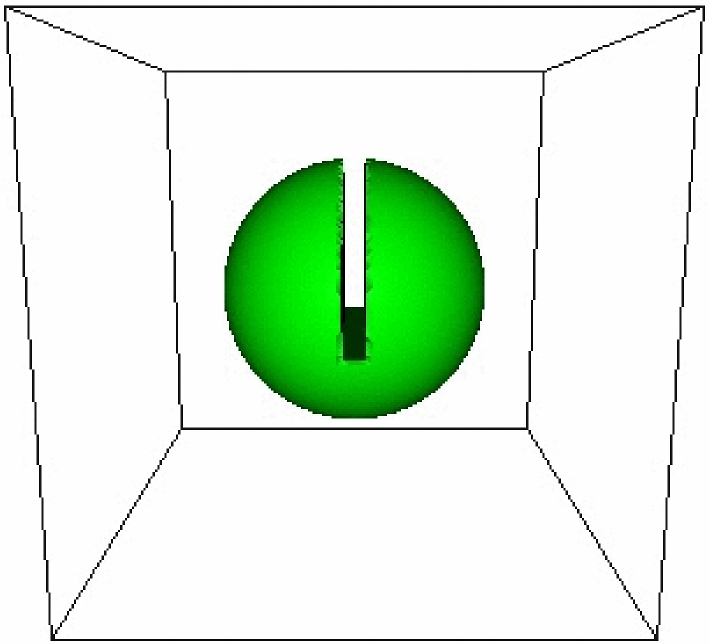

Fifth order level set (WENO) vs. fourth order front tracking (Runge-Kutta)

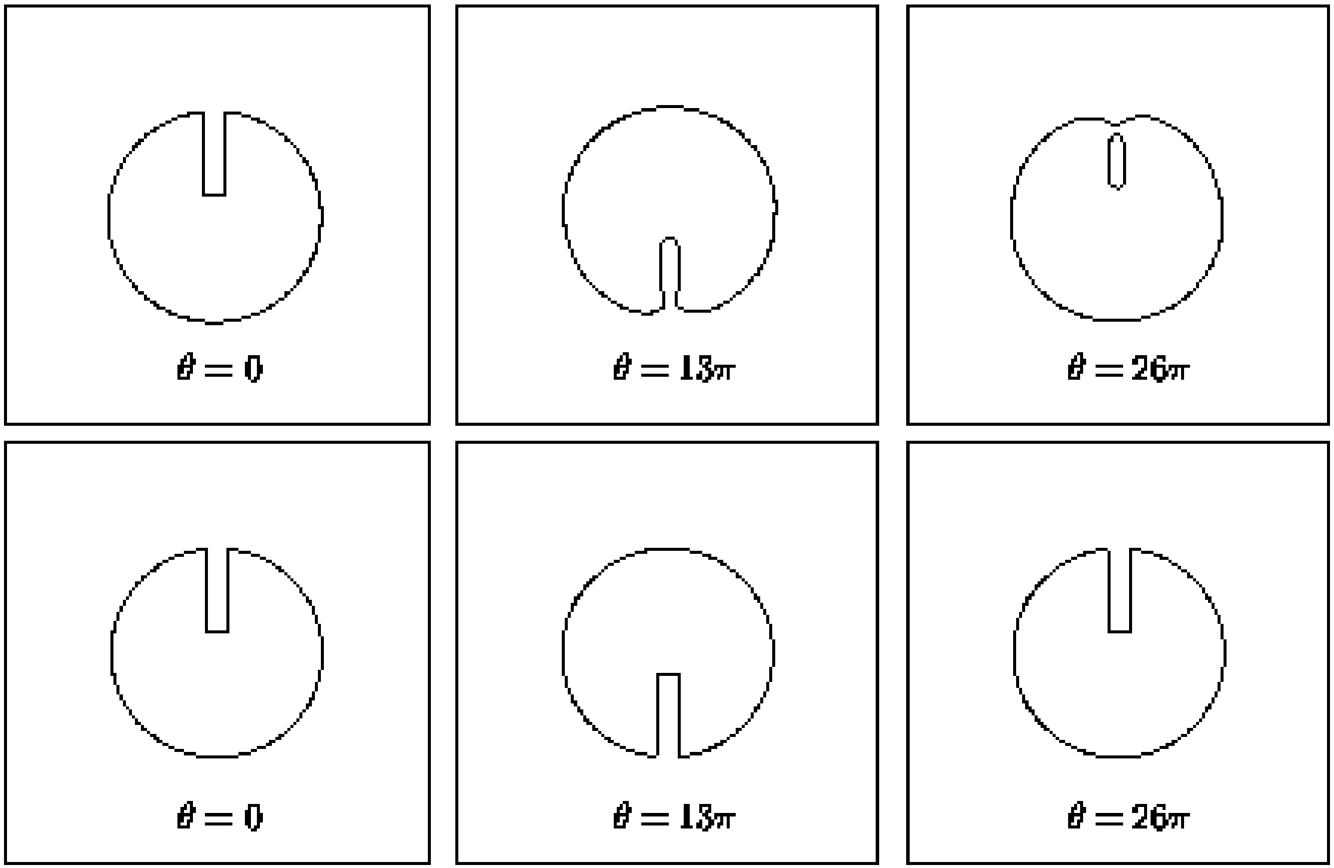

Front tracking reversal test of interface in the deformation velocity field

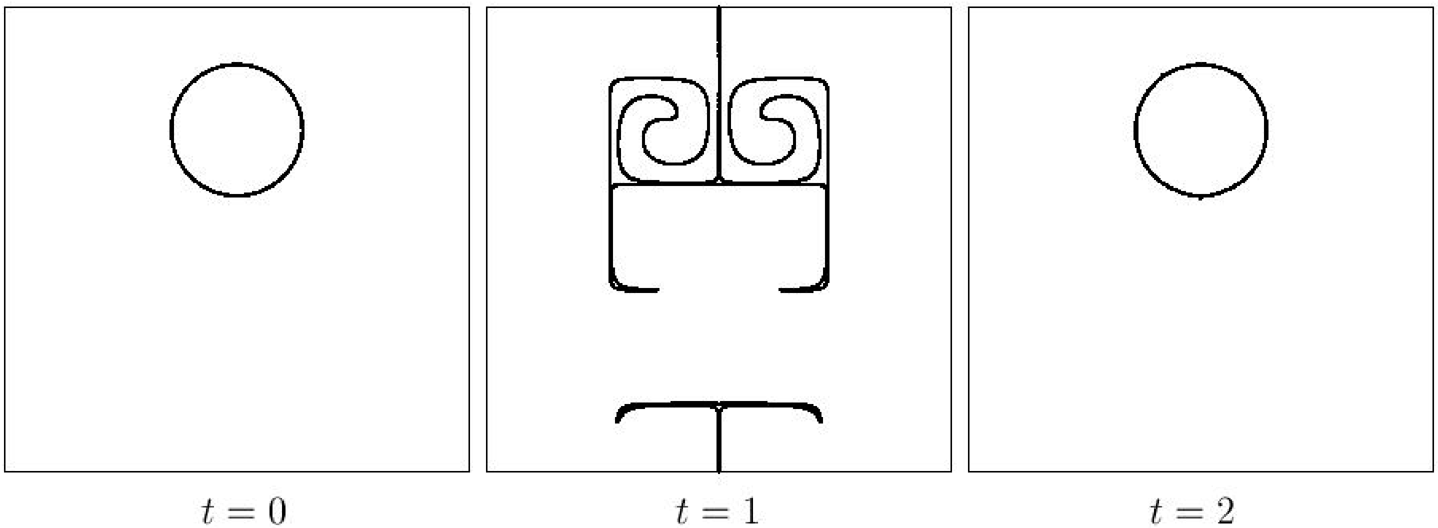

Figure 2: *Reversal test of a 2D interface in the deformation velocity field. The computation is performed in a* 128^2 *computational mesh. In comparison with Rider and Kothe (95), the resolution of the interface matches the best results by the Marker Particle methods.*

Resolution Test

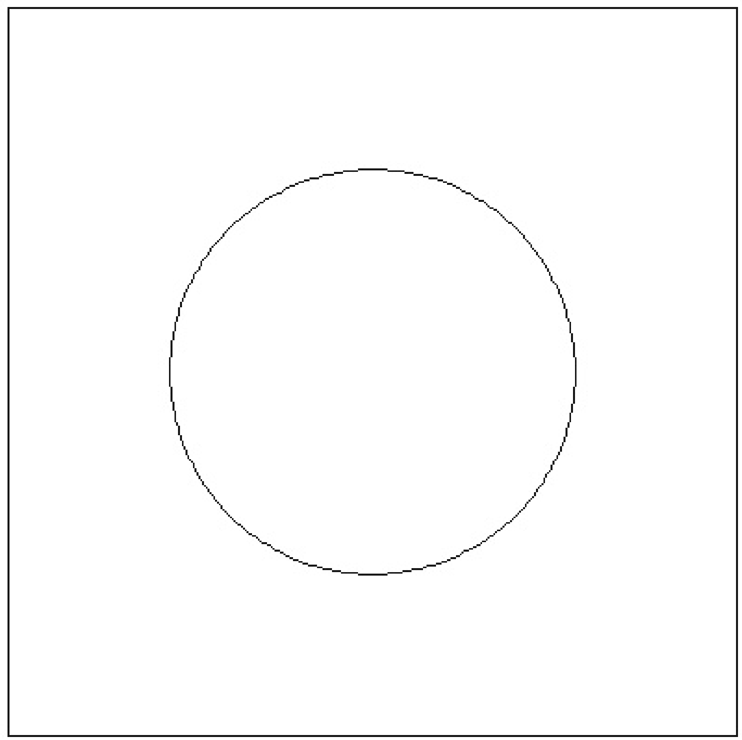

Front tracking reversal test of interface in 3D deformation velocity field

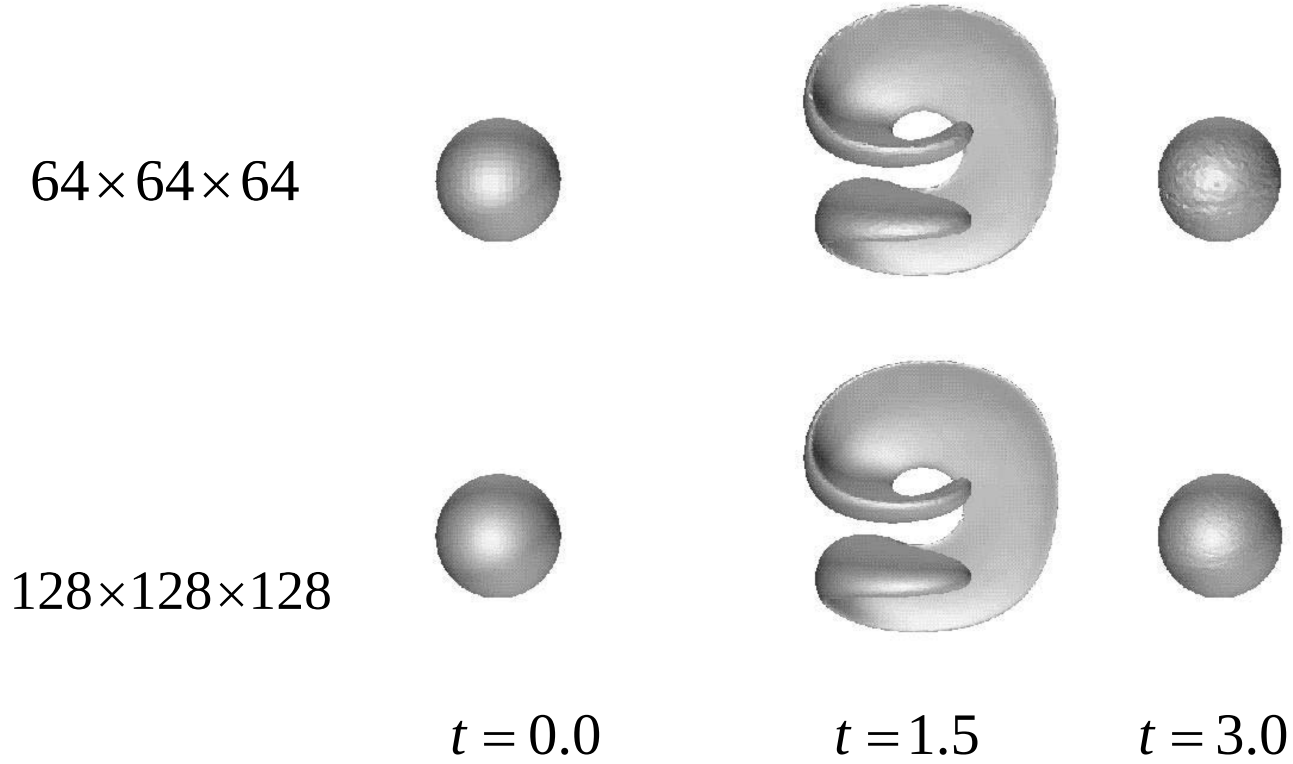

Topological bifurcation: it's done!

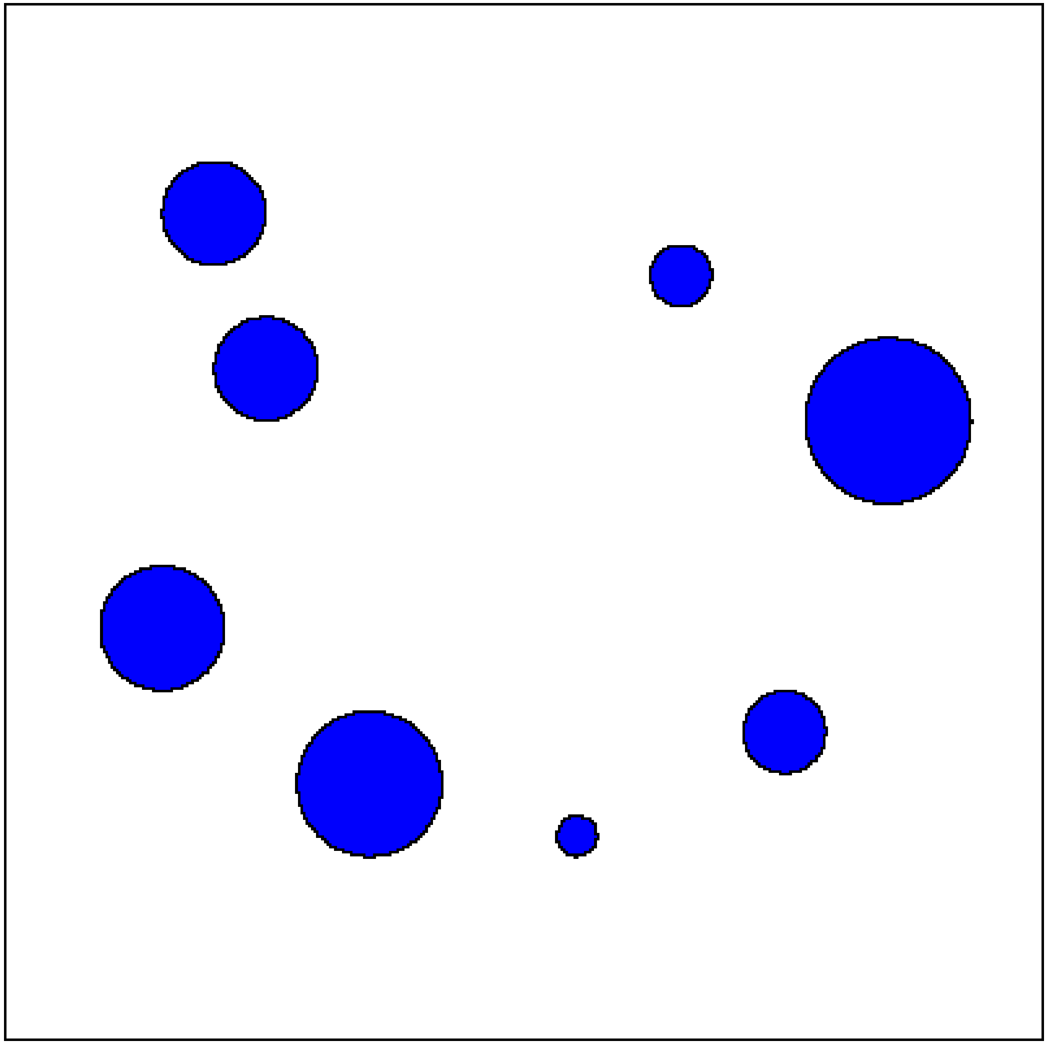

Topological merging of 3D surface mesh

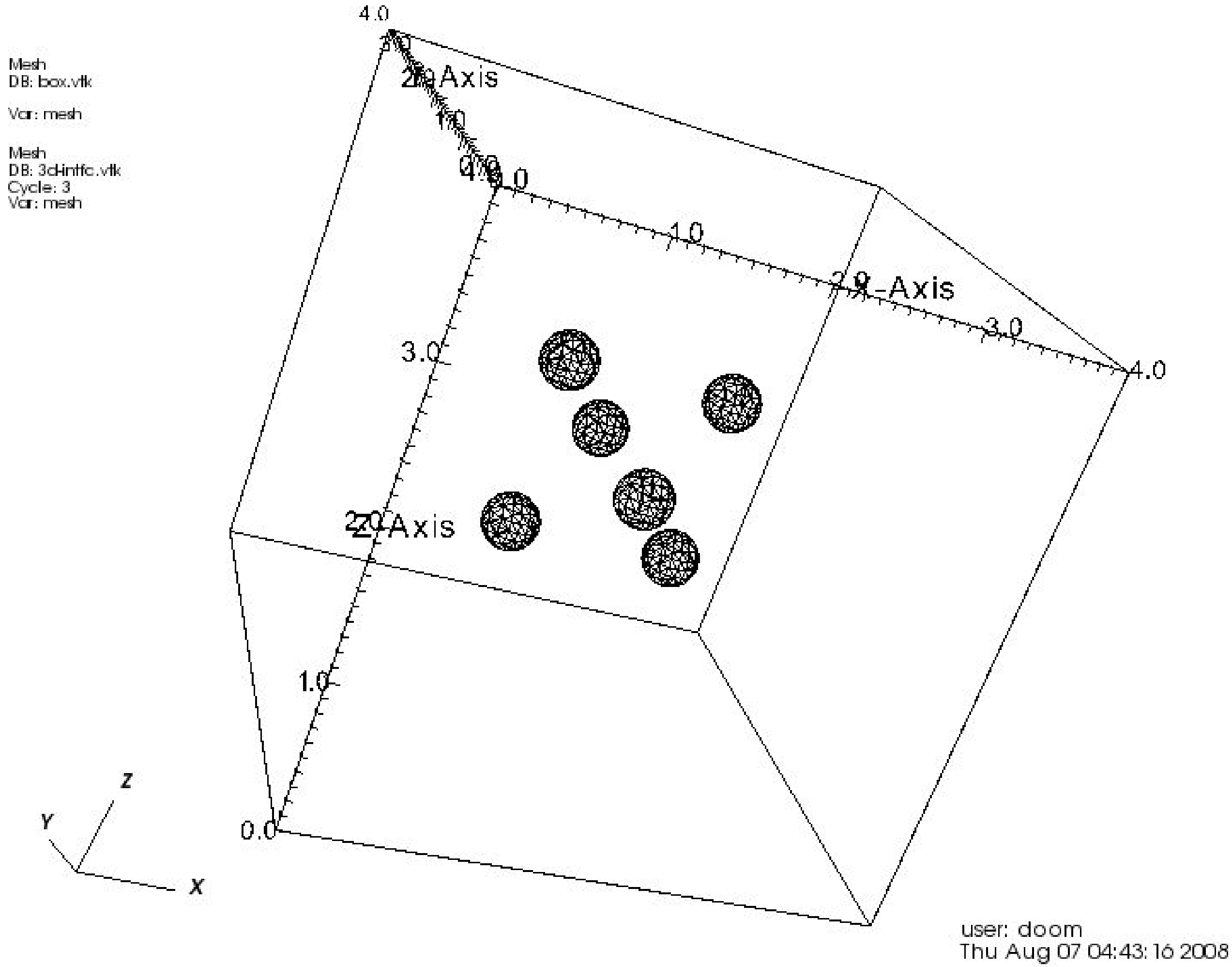

Examples

- Interface bifurcation and merging are commonly observed in multiphase flow

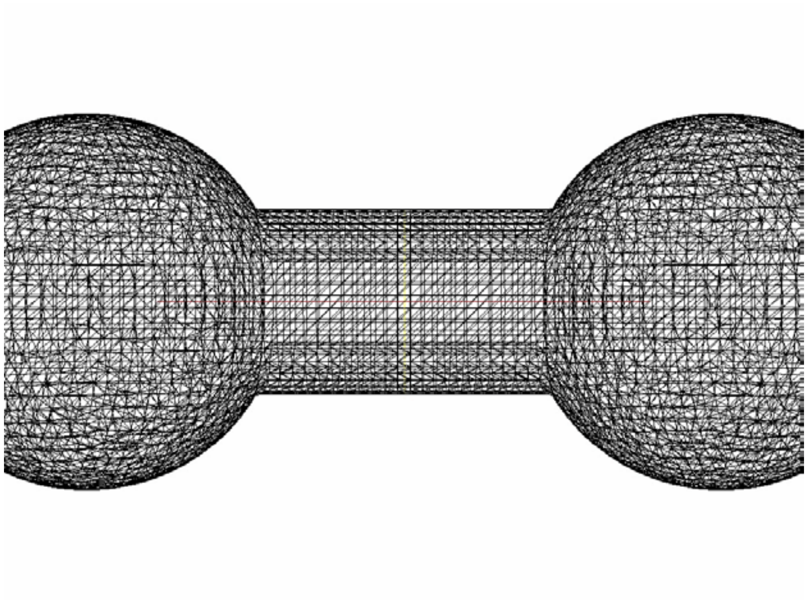

mesh bifurcation in a curvature dependent surface propagation

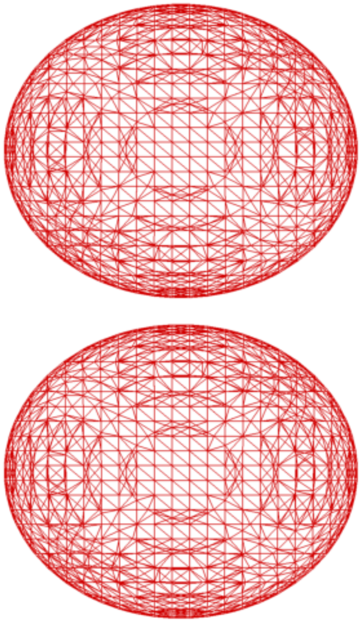

mesh merging in a droplet collision simulation

Conservative Front Tracking

The extended stencil method

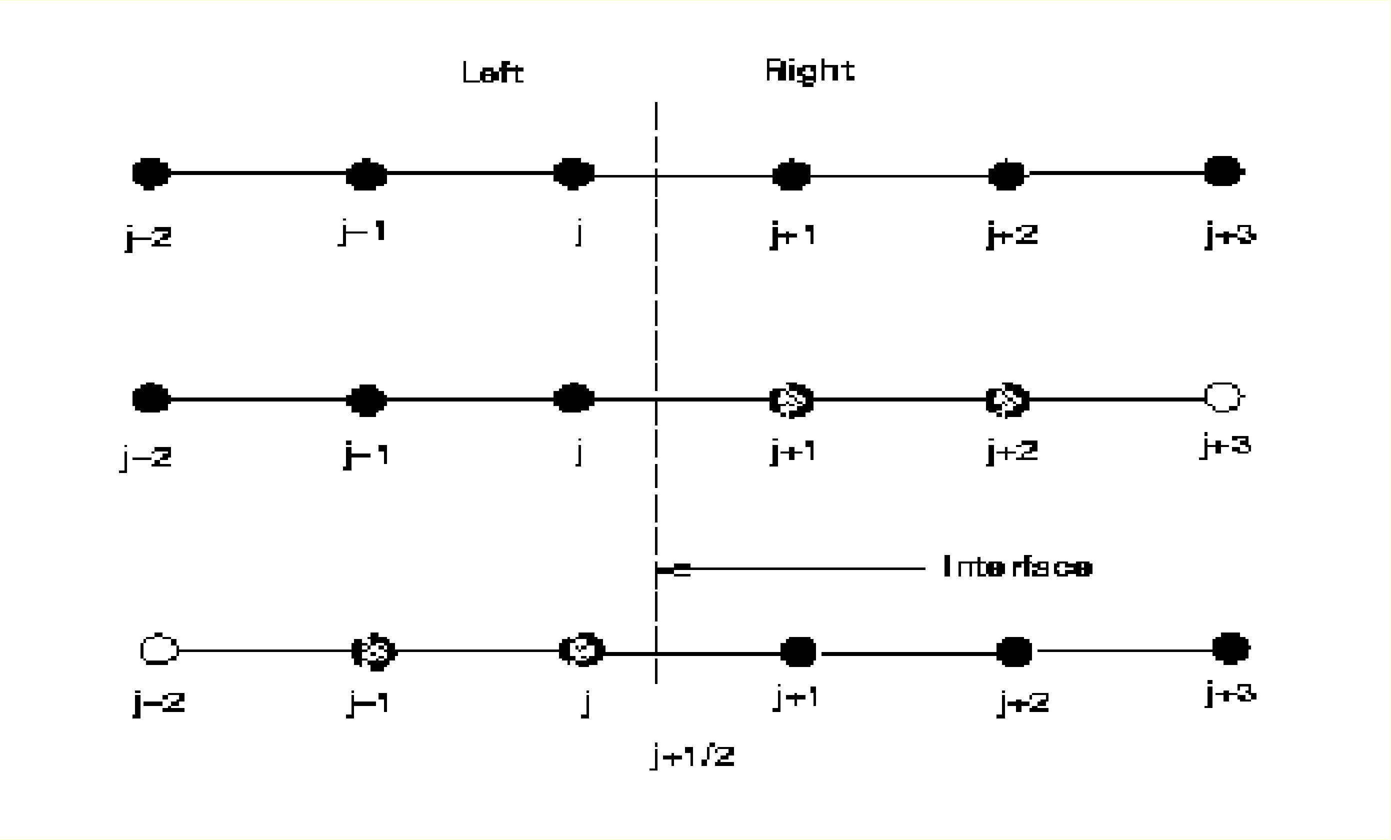

SciDAC
Scientific Discovery through Advanced Computing

For ghost-cell scheme:

$$u_j^{n+1} = u_j^n - \frac{\Delta t}{\Delta x}\left(F_{j+1/2}^L - F_{j-1/2}\right)$$

$$u_{j+1}^{n+1} = u_{j+1}^n - \frac{\Delta t}{\Delta x}\left(F_{j+3/2} - F_{j+1/2}^R\right)$$

$$F_{j+1/2}^L = F(u_{j-1}^n, u_j^n, \overline{u}_{j+1}^n, \overline{u}_{j+2}^n)$$

$$F_{j+1/2}^R = F(\overline{u}_{j-1}^n, \overline{u}_j^n, u_{j+1}^n, u_{j+2}^n)$$

$$F_{j+1/2}^L \neq F_{j+1/2}^R$$

Previous works

1. Chern and Colella, LLNL Report,1987

2. D. K. Mao, JCP, 1991, 1993

3. Pember, JCP, 1995

Neglect higher order term and note that

$$\int_{\Delta V} u dV = \int_{S_M} u v_n dS \Delta t$$

We have the integral form of conservation

$$\frac{\partial}{\partial t}\int_V u dV - \int_{s_M} u v_n dS + \oint_S F_n(u) dS = 0$$

This can also be written as

$$\frac{\partial}{\partial t}\int_V u dV + \int_{S_F} F_n(u) + \int_{S_M} (F_n(u) - v_n u) dS = 0$$

Or simply

$$\frac{\partial}{\partial t}\int_V u dV + \oint_S (F_n(u) - v_n u) dS = 0$$

Conservative Interface-Interior Coupling

The conservation law:

$$u_t + f(u)_x = 0$$

The Rankine-Hugoniot condition:

$$f(u_L) - su_L = f(u_R) - su_R$$

In 1-D, this lead to:

$$\Delta x_j^{n+1} U_j^{n+1} = \Delta x_j^n U_j^n - \Delta t\left(F_I^{n+1/2,L} - F_{j-1/2}^{n+1/2}\right)$$

$$\Delta x_{j+1}^{n+1} U_{j+1}^{n+1} = \Delta x_{j+1}^n U_{j+1}^n - \Delta t\left(F_{j+3/2}^{n+1/2} - F_I^{n+1/2,R}\right)$$

where

$$F_I^{n+1/2,L} = f(u_L^{n+1/2}) - s^{n+1/2} u_L^{n+1/2}$$

$$F_I^{n+1/2,R} = f(u_R^{n+1/2}) - s^{n+1/2} u_R^{n+1/2}$$

$$F_I^{n+1/2,L} = F_I^{n+1/2,R}$$

Due to Rankine-Hugoniot condition

1D Conservative Front Tracking Geometry

Two cases

- **Fronts do not cross the cell center in one time step.**
- **Fronts do cross the cell center in one time step.**

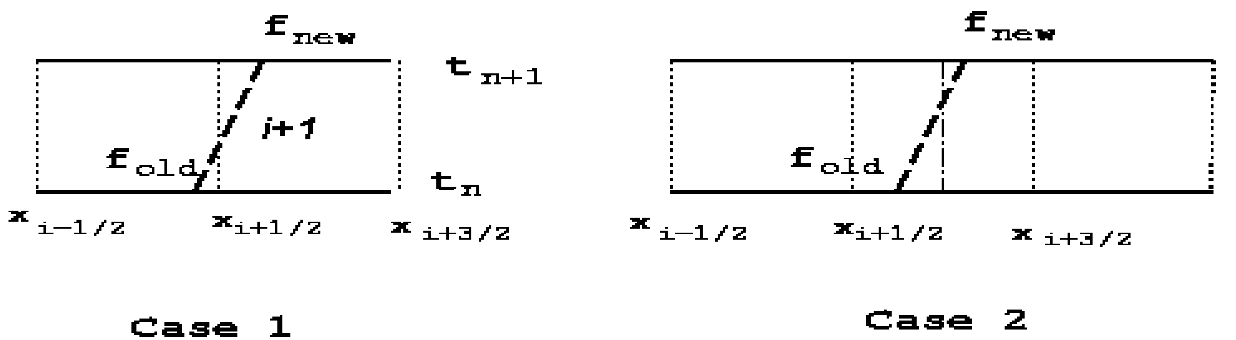

New cell average v_i^n **and** v_{i+1}^n **:**

$$v_i^n = \frac{1}{(\sigma(t_n) - x_{i-1/2})} \int_{x_{i-1/2}}^{\sigma(t_n)} U(x, t_n)\,dx$$

$$v_{i+1}^n = \frac{1}{(x_{i+3/2} - \sigma(t_n))} \int_{\sigma(t_n)}^{x_{i+3/2}} U(x, t_n)\,dx$$

Convergence test of conservative tracking

n (mesh)	shock position error	order	error L1	order
50	4.8e-2		0.481530	
100	1.3e-4	8.5	0.034279	3.8
200	4.3e-5	1.6	0.013060	1.4
400	1.6e-6	1.4	0.004242	1.6

In multi-dimensional case, we consider the time space equation:

$$\vec{F} = u\hat{n}_t + f(u)\hat{n}_x + g(u)\hat{n}_y + h(u)\hat{n}_z \qquad \nabla \cdot \vec{F} = 0$$

On a time-space cell

$$\oint_{TS} \vec{F} \cdot \hat{n}_{ts} dS_{ts} = 0$$

Cell-merge is needed if the volume of the time-space cell is less than half of the regular cell, in 2-D the time space cell is constructed the same way as the 3-D grid based interface.

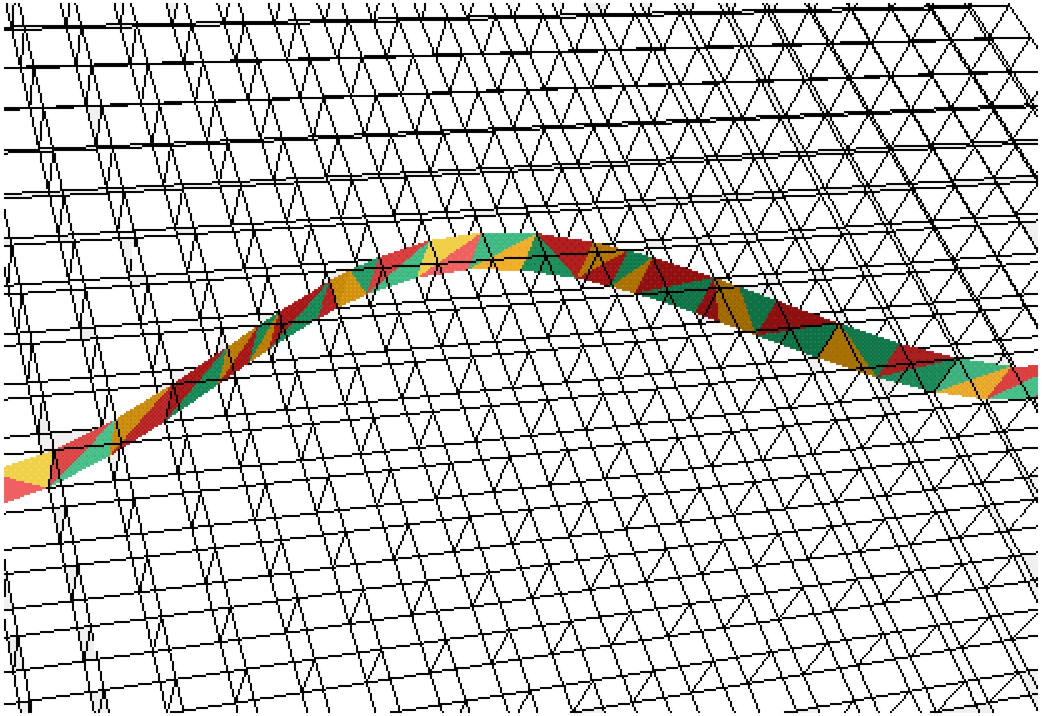

The time-space interface between
n and n+1 time steps

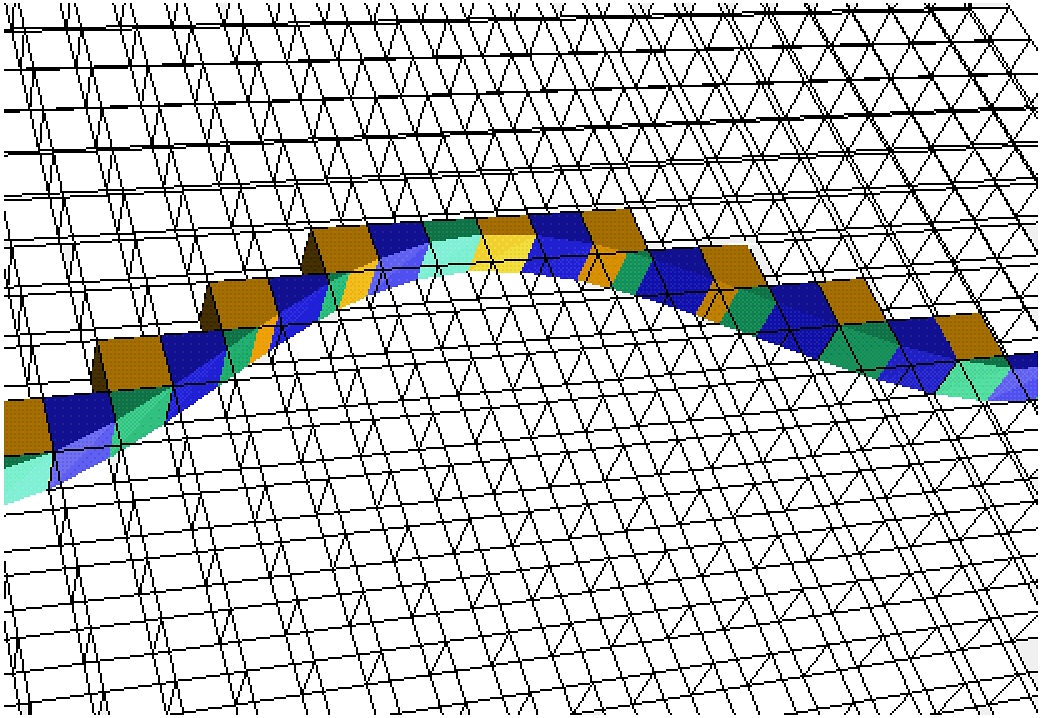

Before cell merger

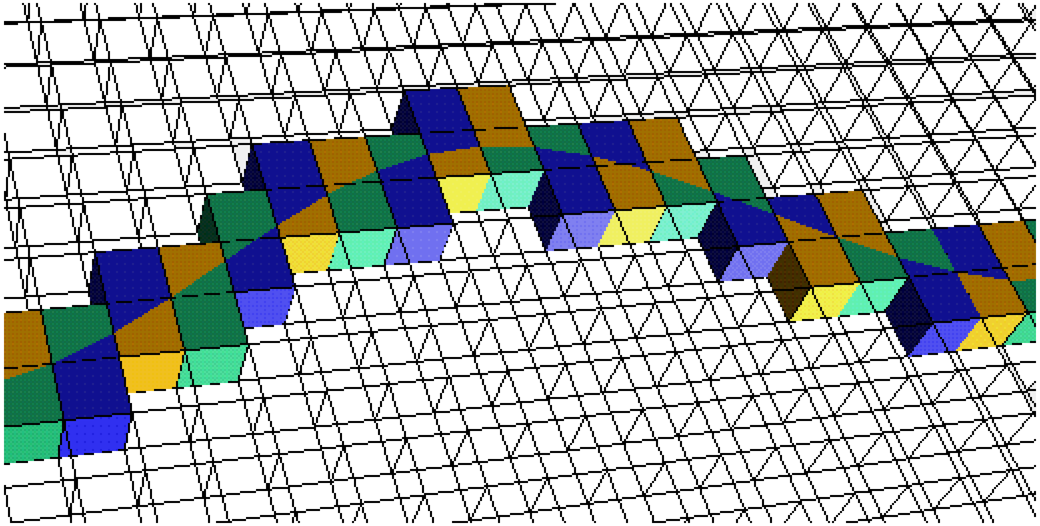

After cell merger

	Conservative Tracking	Nonconsertive Tracking
Mass Error	0.0	0.21%
X-Mom Error	0.0	0.21%
Energy Error	0.0	0.21%

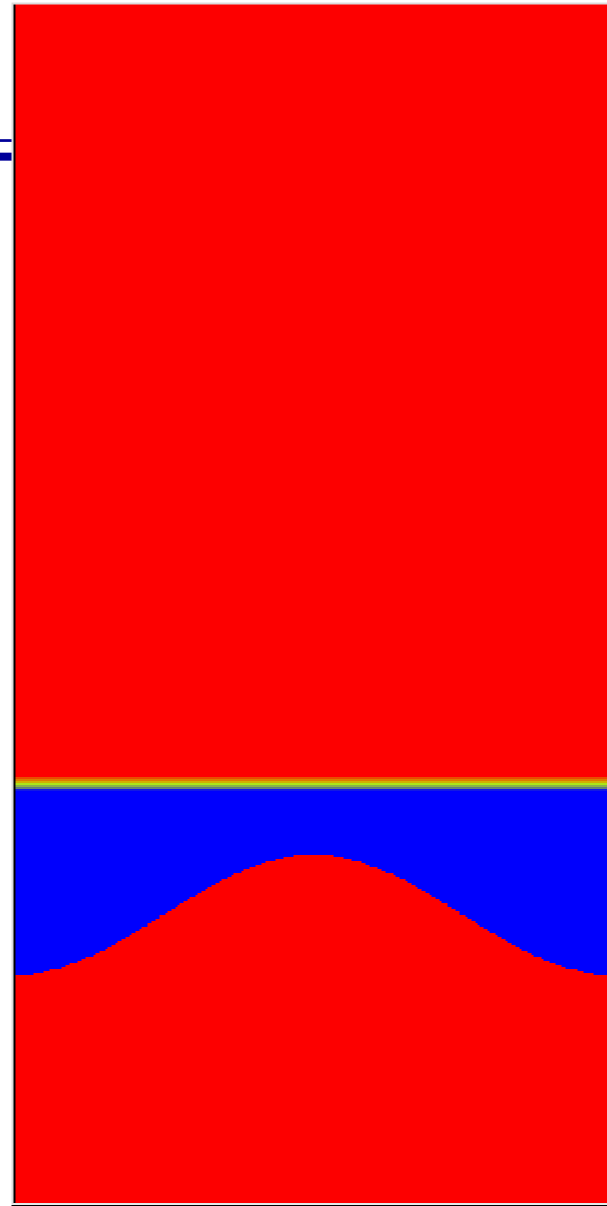

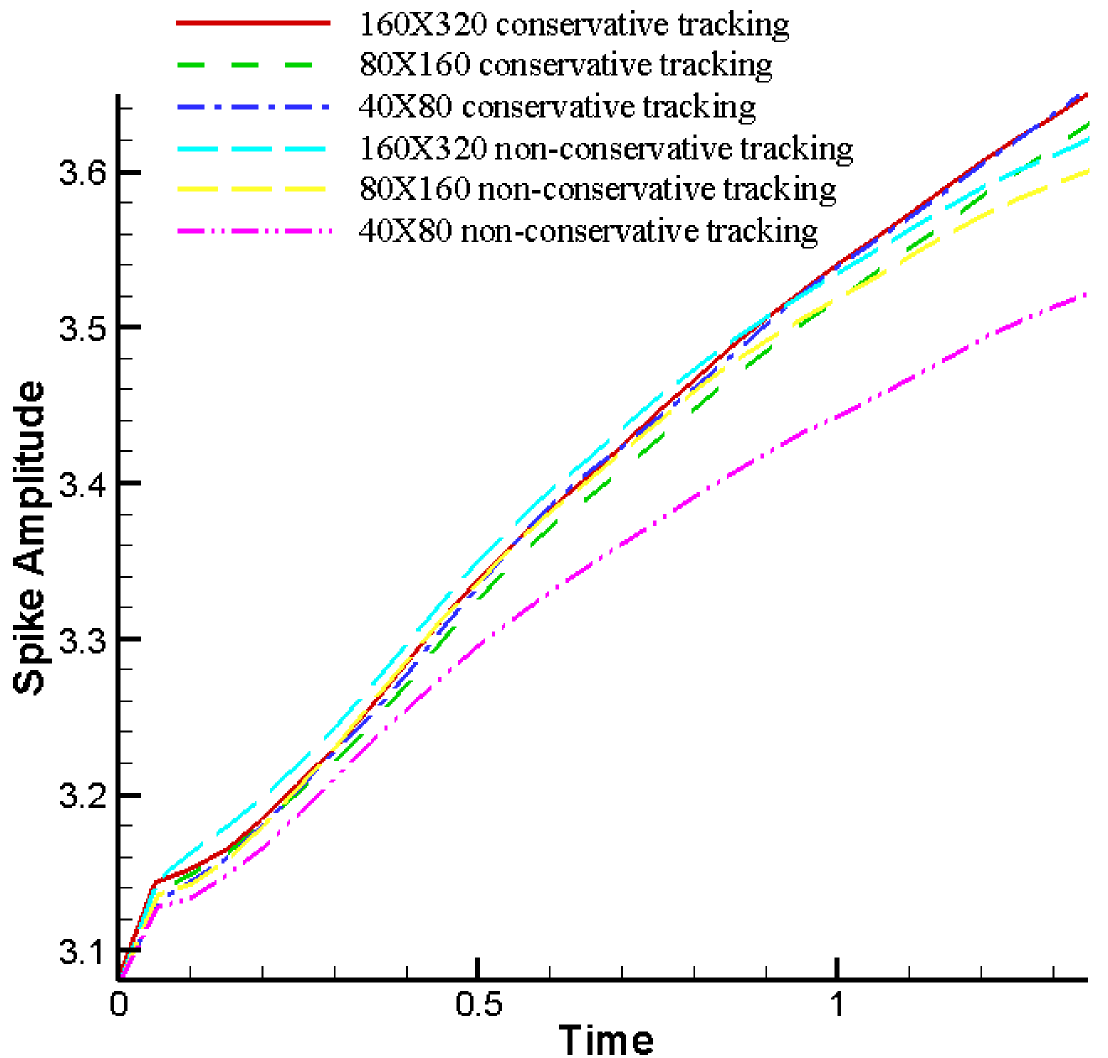
160X320 conservative tracking
80X160 conservative tracking
40X80 conservative tracking
160X320 non-conservative tracking
80X160 non-conservative tracking
40X80 non-conservative tracking
Spike Amplitude
3.1
3.2
3.3
3.4
3.5
3.6
Time
0
0.5
1

Rayleigh-Taylor Instability

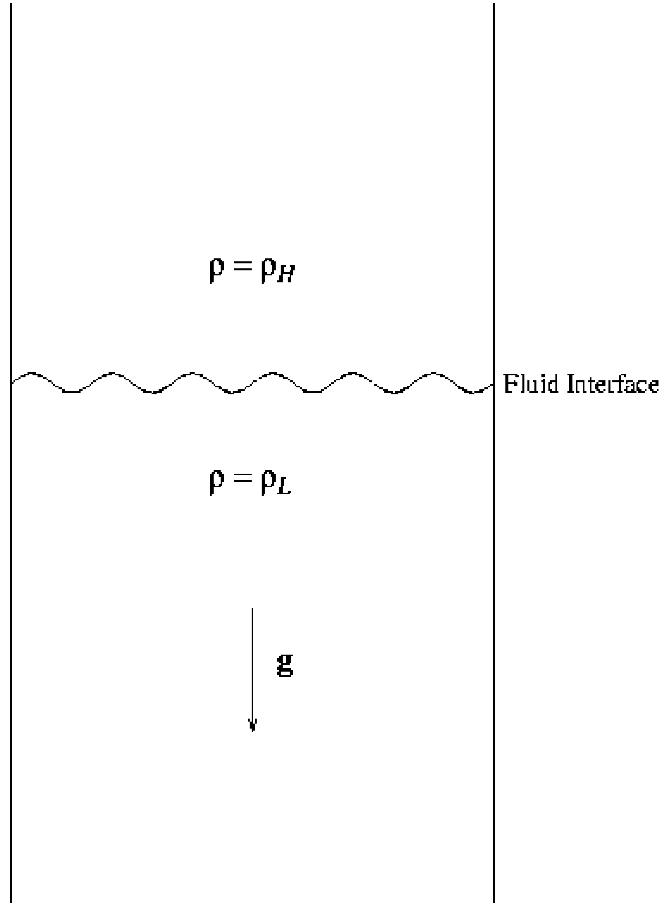

Inertial Confinement Fusion (ICF)

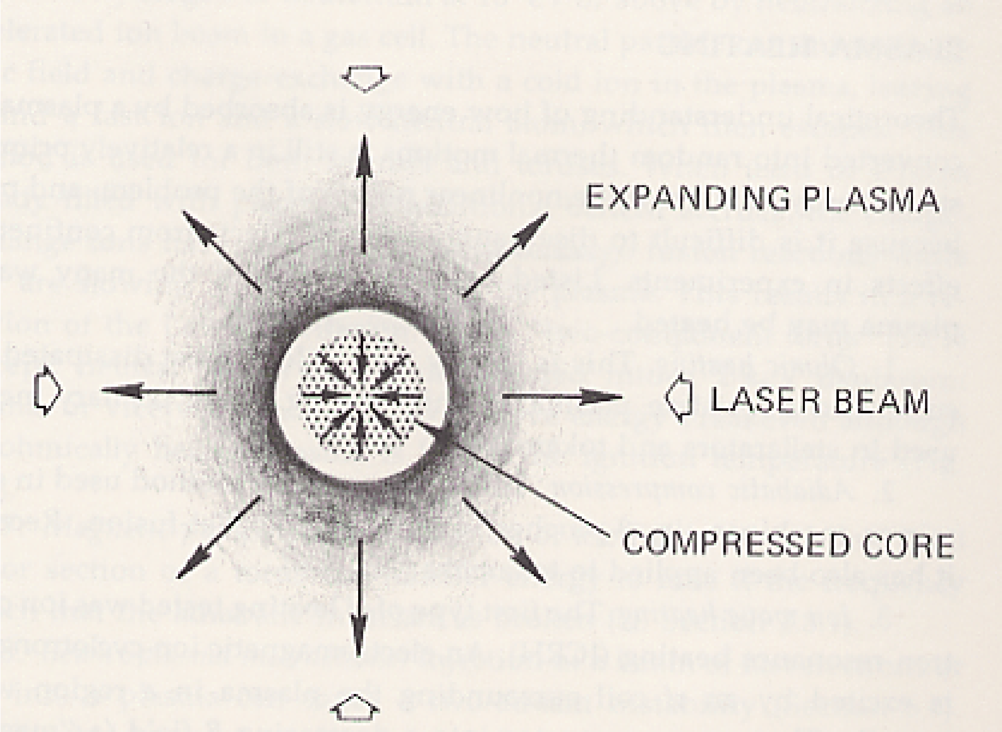

FronTier application: chaotic mixing

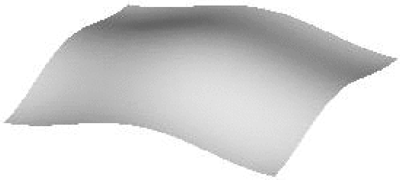

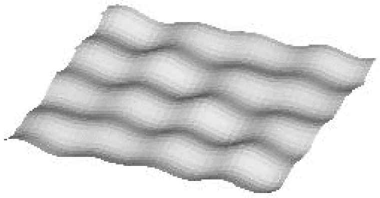

Scientific Discovery through Advanced Computing

FronTier application: chaotic mixing

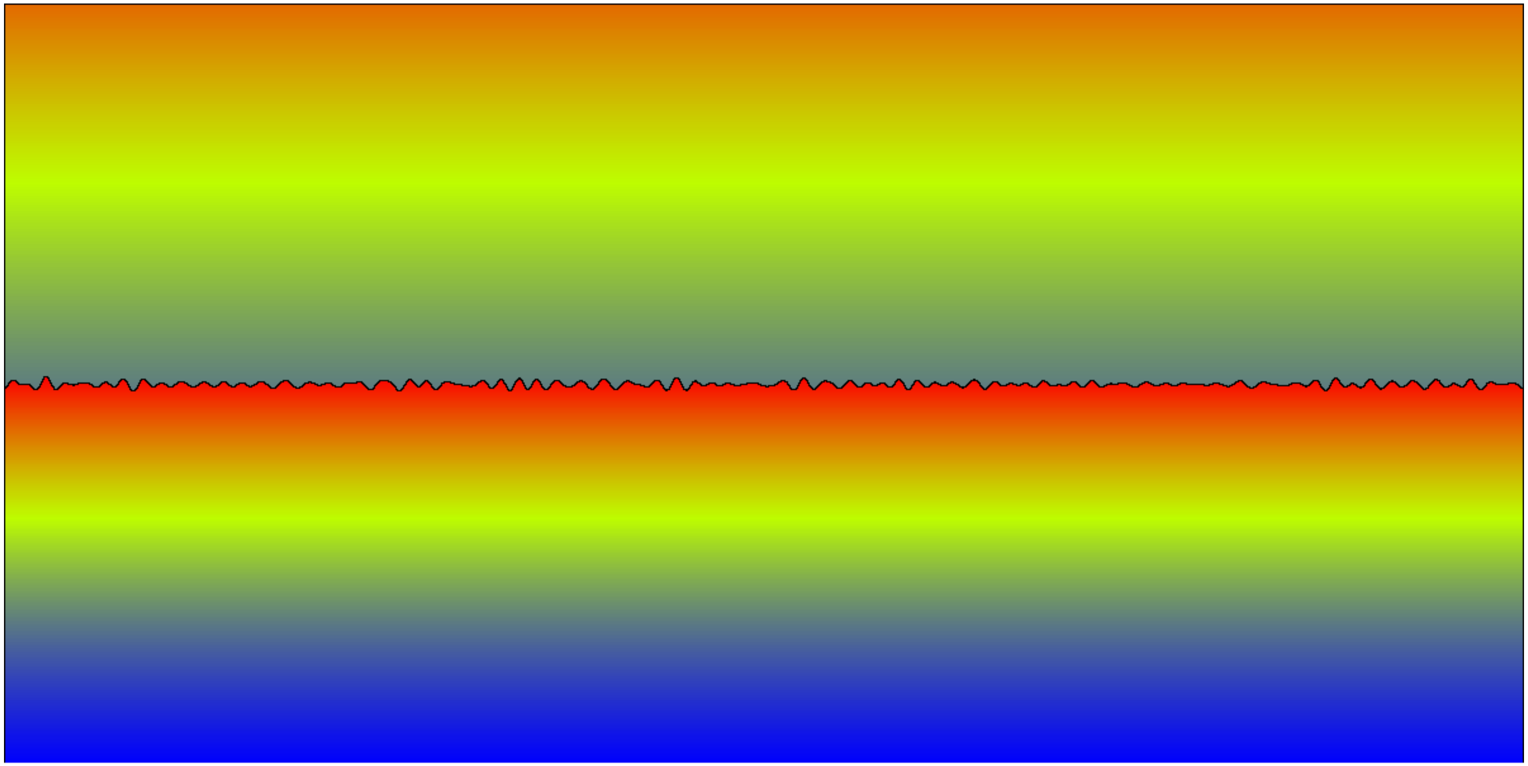

Chaotic mixing is not only important to ICF, but also a test of large scale FronTier application to petascale computing. We have implemented a load balanced parallel algorithm and ran up to 1024 processors on New York Blue. Collaboration with B. Cheng, John Grove, and D. Sharp at LANL.

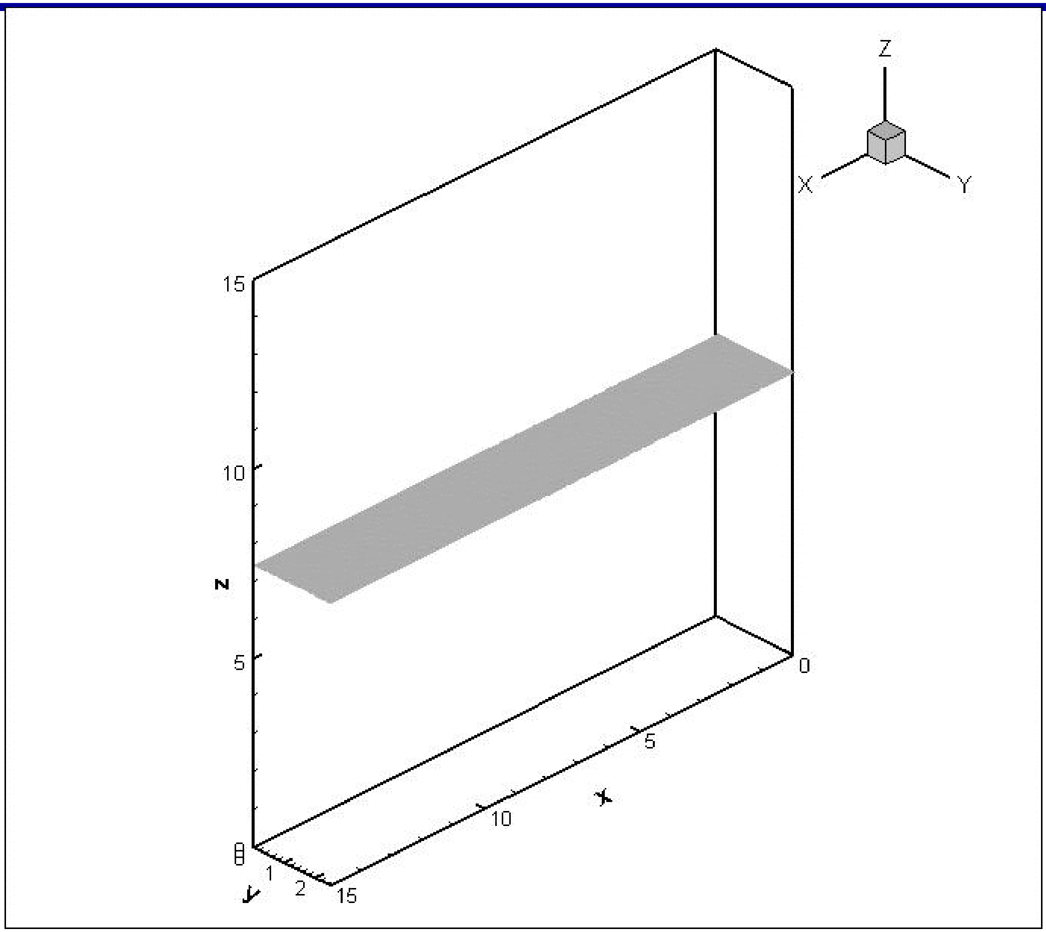

Z
X
Y
15
10
5
0
z
x
y
0
5
10
15
1
2

Acceleration Driven Mixing

- Rayleigh-Taylor (RT), steady acceleration:

$$h = \alpha A g t^2 ; A = \frac{\rho_2 - \rho_1}{\rho_2 + \rho_1}$$

The α Paradox

$$h_b = \alpha A g t^2$$

David Youngs and K.Read
(1984)

Read’s Experiment (1984)

3D alcohol/air	Exp # 29	Alpha = 0.073
	39	0.076
	58	0.077
3D NaI soln./Pentane	Exp # 33	Alpha = 0.066
	35	0.071
3D NaI soln./Hexane	Exp # 62	Alpha = 0.063
	60	0.073

Summary of Experiments

Experiments			
Read/Youngs	'84	$\alpha_b \sim 0.58 - 0.65$	2D
		$\alpha_b \sim 0.063 - 0.077$	3D
Kucherenko	'91	$\alpha_b \sim 0.07$	3D
Snider/Andrews	'94	$\alpha_b \sim 0.07 \pm 0.007$	3D
Schneider/Dimonte/Remington	'99	$\alpha_b \geq 0.054$	3D
Dimonte/Schneider	'99	$\alpha_b \sim 0.05 \pm 0.01$	3D

The Alpha of Bubbles

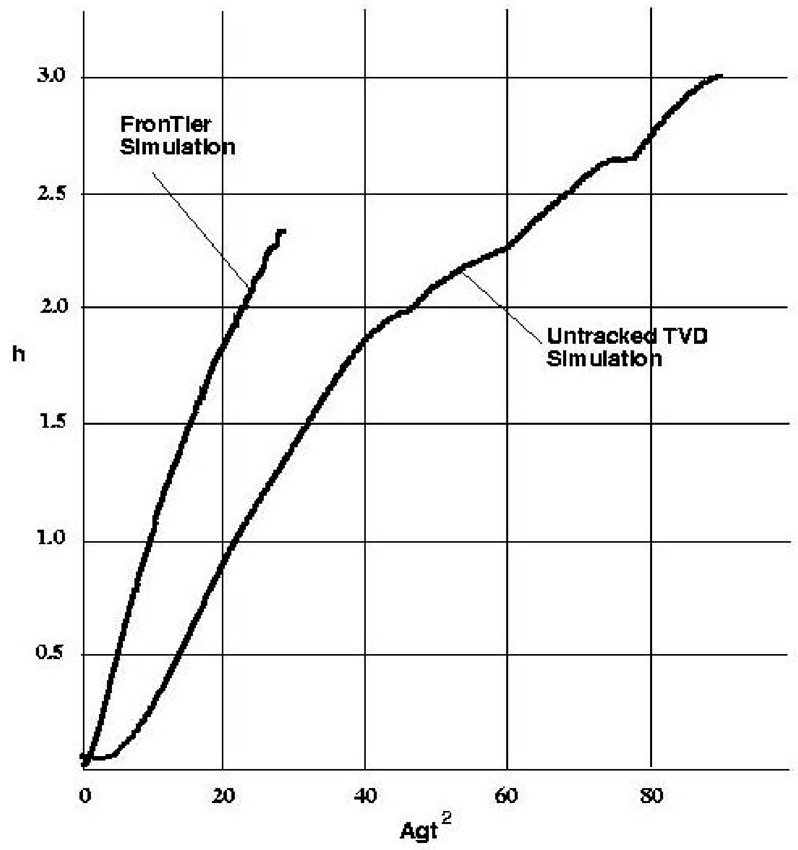

FronTier:
Alpha = 0.08

TVD:
Alpha = 0.025-0.045

FronTier

TVD

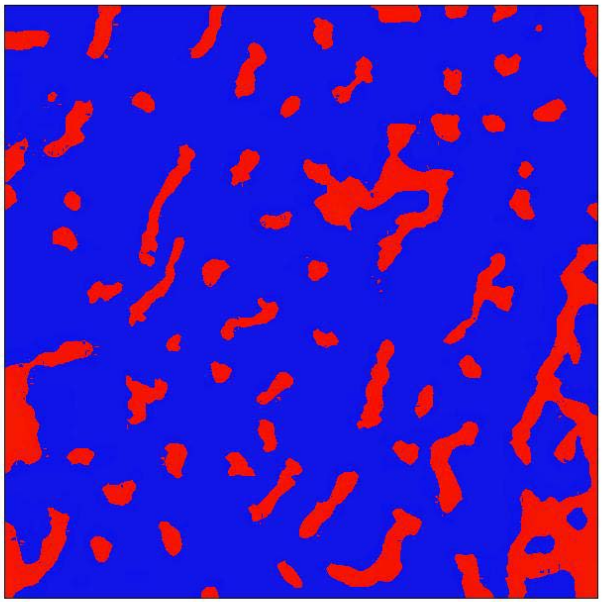

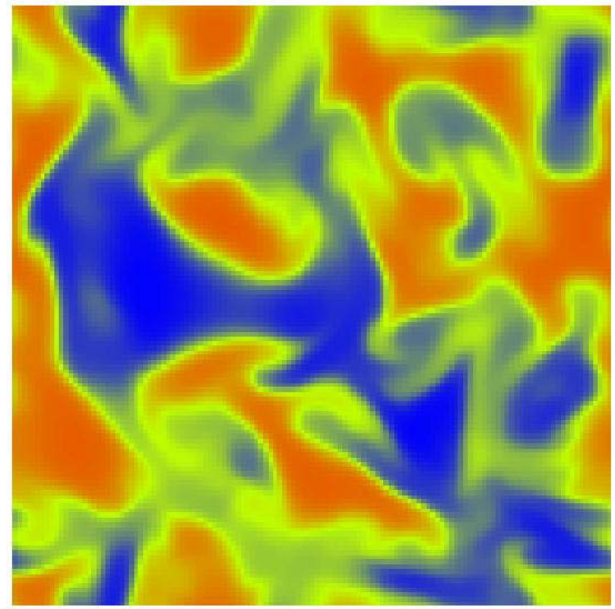

$Agt^2 = 25.3$ $h = 4.16$ Density plot

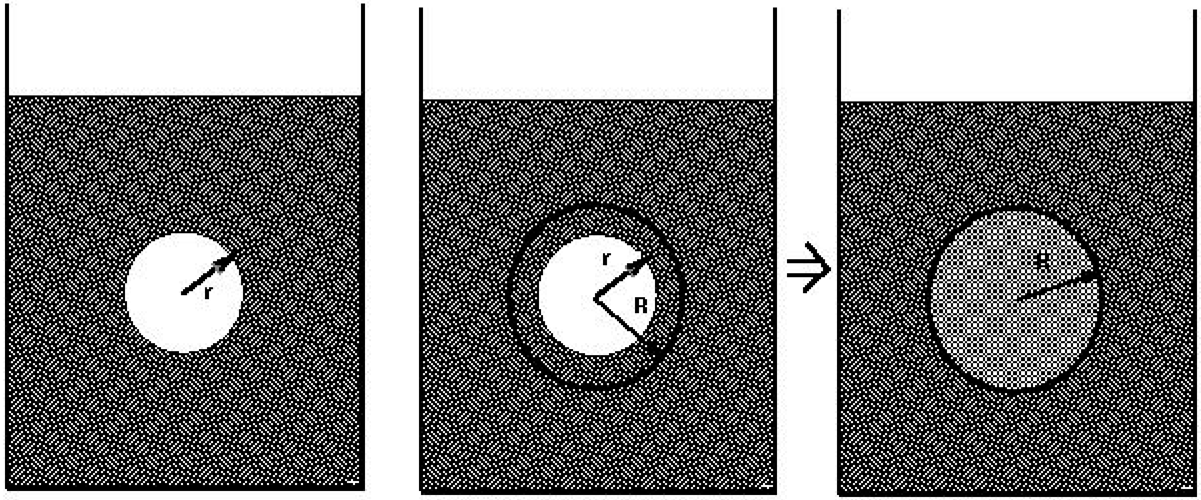

(a) (b) (c)

$$M_1 = \frac{4\pi}{3} r^3 \rho_L \qquad M_2 = \frac{4\pi}{3} \rho_L + \frac{4\pi}{3} (R^3 - r^3) \rho_H$$

$$f_1 = f_2 = \frac{4\pi r^3}{3} (\rho_H - \rho_L) g$$

$$a_1 = \frac{\rho_H - \rho_L}{\rho_L} g \qquad a_2 = \frac{\rho_H - \rho_L}{\rho_L + \left(\frac{R^3}{r^3} - 1\right) \rho_H} g$$

Goal of mixing study

- Predict large scale features. Size of mixing zone
- Predict statistics (means, variances) of fluid quantities
- For use in combustion
  - Predict full probability distribution (PDF) of species concentration and temperatures
- Accurate models down to atomic level of mix are needed
- These must be sensitive to transport, Reynolds number, Schmidt number

Real vs. Ideal Mixing Physical vs. Numerical Scale Breaking

- Numerical nonideal effects
  - Numerical surface tension
  - Numerical mass diffusion
- Physically nonideal effects
  - Surface tension
    - Surfactants, variable surface tension, Marangoli force
  - Mass diffusion
    - Initial or for all times
  - Viscosity
  - Compressibility
  - Long wave length initial perturbations

Main New Results

- Systematic agreement of simulation with experiment and theory
- **Alpha, bubble width, bubble height fluctuations**
  - **Most relevant experiments included in agreement**
    - Reed-Youngs, Smeeton-Youngs, Andrews experiments
    - Omitted:
      - Immiscible with surfactant (Dimonte and Smeeton-Youngs)
      - Initial diffusion layer (in progress)
      - Subgrid models
      - Nonideal initial conditions

Scale Breaking: Experiments and Simulations

Scale breaking physics	Alpha-experimental	Alpha-simulation	Experiments	Fluids
Surface tension	0.050-0.077	0.067	RY, SY	Liquid/liquid; liquid/gas
Surface tension with surfactant	0.050-0.061	????	SY,DS	Liquid/liquid
Mass diffusion	0.070	0.069	BA	Gas/gas
Initial mass diffusion	0.062	????	SY	Liquid/liquid
Viscosity	0.070	????	SA	Liquid/liquid
Compressibility		Up to 0.2	Lasers	plasmas

SciDAC Scientific Discovery through Advanced Computing

Comparison of Mixing Rates: Comparison, Simulation and Theory

	Theory	Experiment	Simulation
height	0.06	0.067	0.062
radius	0.01	0.01	0.01
fluctuations in height		0.028	0.034

Turbulent Mixing

- Acceleration driven mixing
  - Steady acceleration – Rayleigh-Taylor mixing
  - Impulsive acceleration – Richtmyer-Meshkov mixing
- Most RT computations underpredict mixing rates relative to experiments
  - Simulation analysis using time dependent densities (Atwood number) makes this point
- Cause appears to be numerical mass diffusion, which reduces the local density contrast and thus the large scale mixing rates
  - Numerical surface tension also significant
- Questions raised about the role of initial noise in the experiments

Numerical Non-Ideal Effects

- Numerical mass diffusion
  - Removed by tracking
  - Errors modify density contrast by a factor of 2 for typical grids
- Numerical surface tension
  - Reduced by local grid based (LGB) tracking
  - Errors proportional to curvature x Delta x
  - Arises from approximation of interface by a line segment within each mesh block
  - Arises from grid level description of interface and thus occurs for all untracked methods

Time Dependent Atwood Number

- Atwood number
- For each z

$$A = \frac{\rho_2 - \rho_1}{\rho_2 + \rho_1}$$

  – Compute the maximum and minimum density
  – Form a space (height) and time dependent A(z,t) from min/max
- Average A(z,t) over bubble region to get A(t)
- Untracked A(t) is about ½ nominal value due to mass diffusion; (incompressible) tracked A(t) is virtually constant
- If A(t) is used in definition of alpha, all low compressible simulations agree (with each other, with experiment, with theory)
- If A(t) is used in compressible simulations, all simulations are self similar, but self similar growth rate depends on compressibility

Physical Non-Ideal Effects

- Viscosity, mass diffusion, surface tension
- Compressibility
  - Solution depends on initial temperature stratification; assume isothermal. Initial density depends on height z, so that Atwood number is z dependent.
  - Data interpretation using a time dependent Atwood number restores self similarity, but the mixing rate alpha increases with compressibility.

Turbulent Mixing: Predictions of Gross Features (Mixing Rate alpha, etc.)

- Systematic agreement of theory, simulation and experiment for RT turbulent mixing
  - Scale breaking physics important to this agreement
- Tracking is the best of practical interface methods
  - Control over numerical mass diffusion and numerical surface tension needed for RT agreement
- Validation studies still in progress (viscosity)

Other Applications of Front Tracking

Ask not what the earth can do for us, ask what we can do for the earth

American consumes about 200 billion gallons per year, a 10% saving will be 20 billion gallon amounts to more than 40 billion dollars, not to mention the benefit to the environment.

3D Simulation of a Real Fuel Injection

- All parameters are from an experiment performed by Parker*

nozzle radius (R)	0.1mm	Reynolds number	20,300
grid	20/R	Weber number	2.2×10^6
fuel density	0.66 g/cm^3	Ohnesorge number	0.073
gas density	0.0165 g/cm^3	Density ratio	40
fluid viscosity	0.013 Poise		
surface tension	24 mN/m^2		

* P. Parker, *Atomization and Sprays*, 8, (1998)

Verification: Rayleigh Instability

Comparison with the dispersion relation

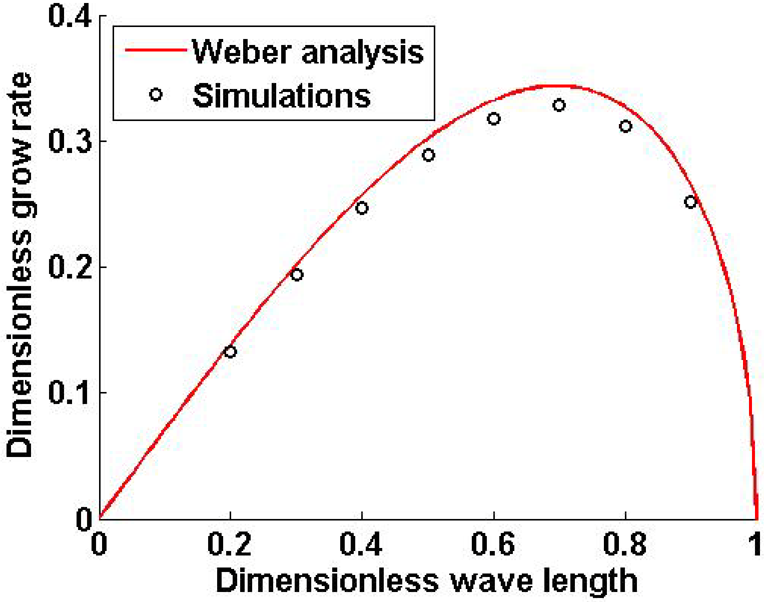

The relative errors of the growth rate

Number of cells on radius	FT/GFM (2D)	FT/GFM (3D)
5	0.1396	0.2853
10	0.0607	0.1702
20	0.0321	0.0672

dispersion relation

$$\beta^2 = \frac{\sigma k}{\rho a^2}(1 - k^2 a^2)\frac{I_1(ka)}{I_0(ka)}$$

ρ liquid density
a jet diameter
I_i modified Bessel functions of the first kind
k wave number
σ surface tension coefficient
β growth rate

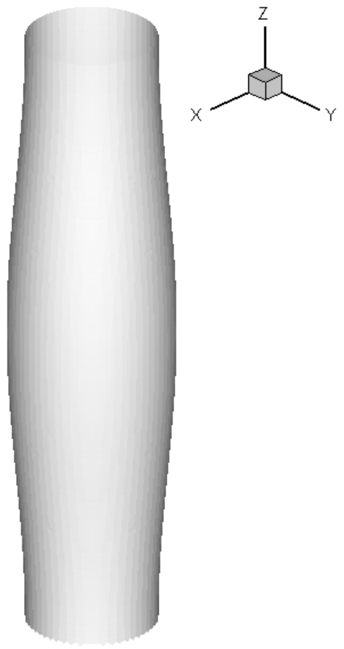

Incompressible fluid equation

$$\mathbf{u}_t + (\mathbf{u}\nabla \cdot \mathbf{u}) = -\nabla p + \nu\nabla^2\mathbf{u}$$

$$\nabla \cdot \mathbf{u} = 0$$

This is a mixed hyperbolic and elliptic equation

U is the velocity of fluid and *p* is the pressure.

Incompressible Rayleigh-Taylor instability on Reynold number (from left: 14,140,1400)

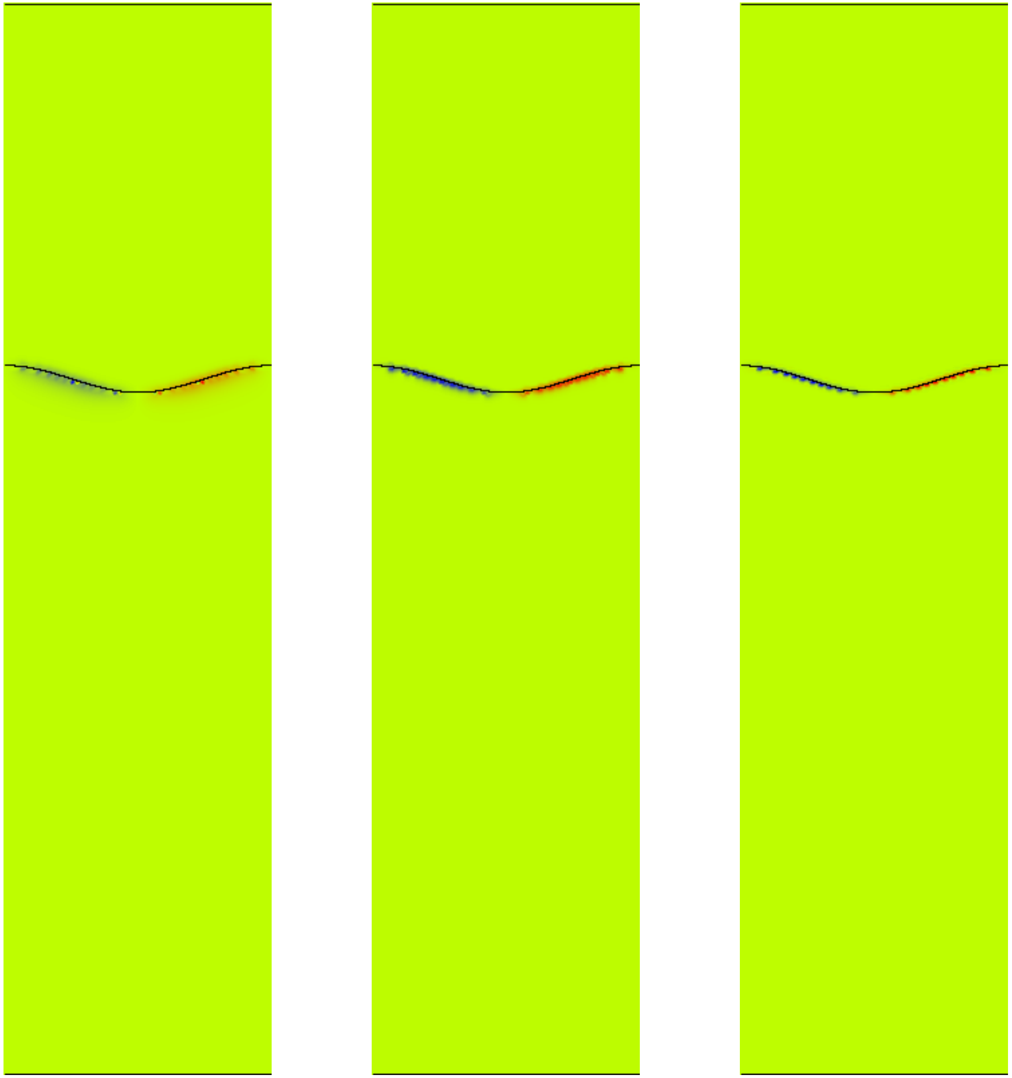

Incompressible code in 3D

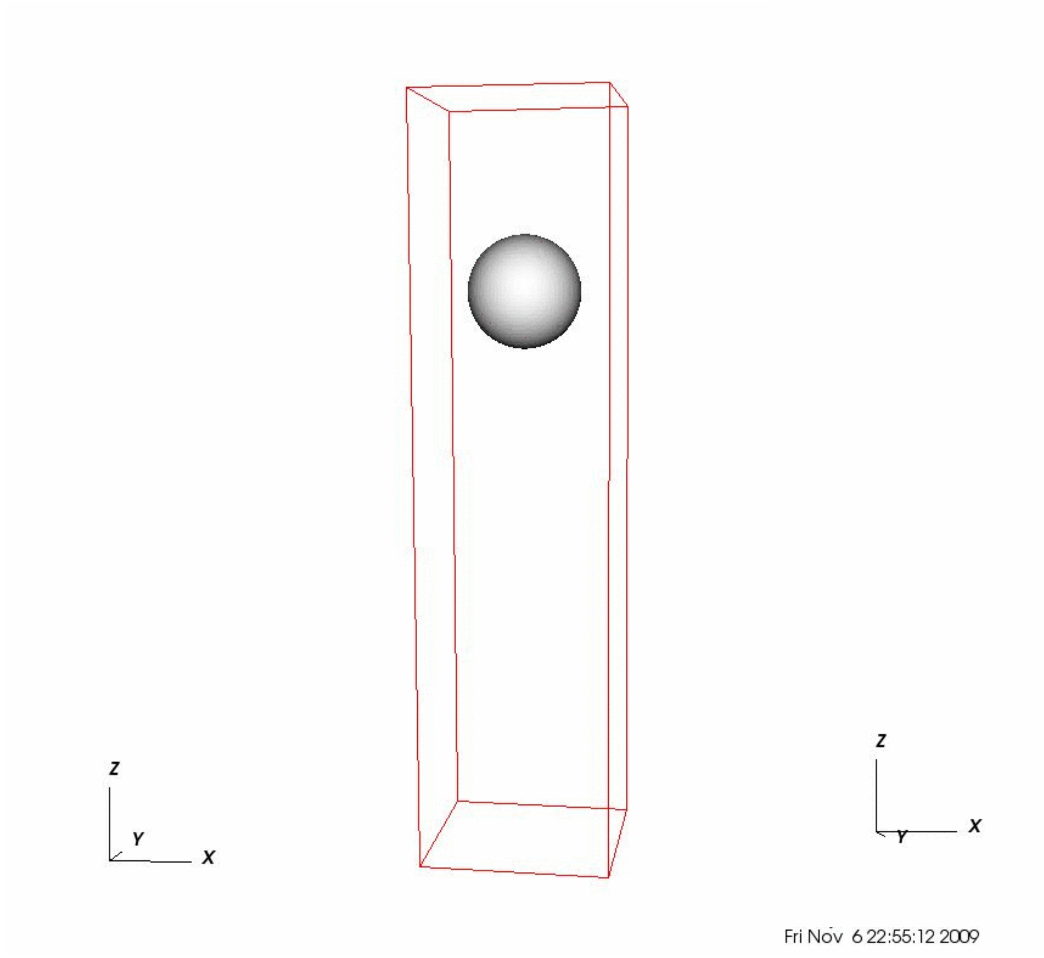

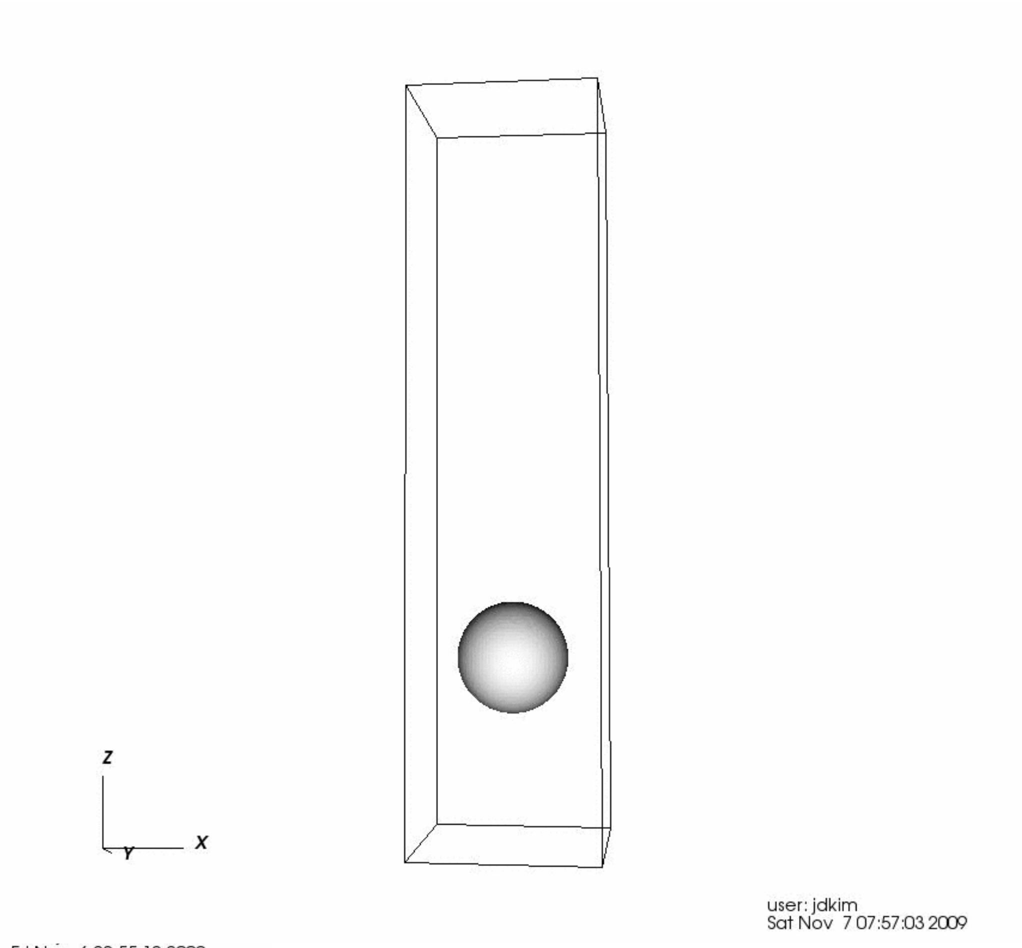

Two Dimensional Solute Precipitation

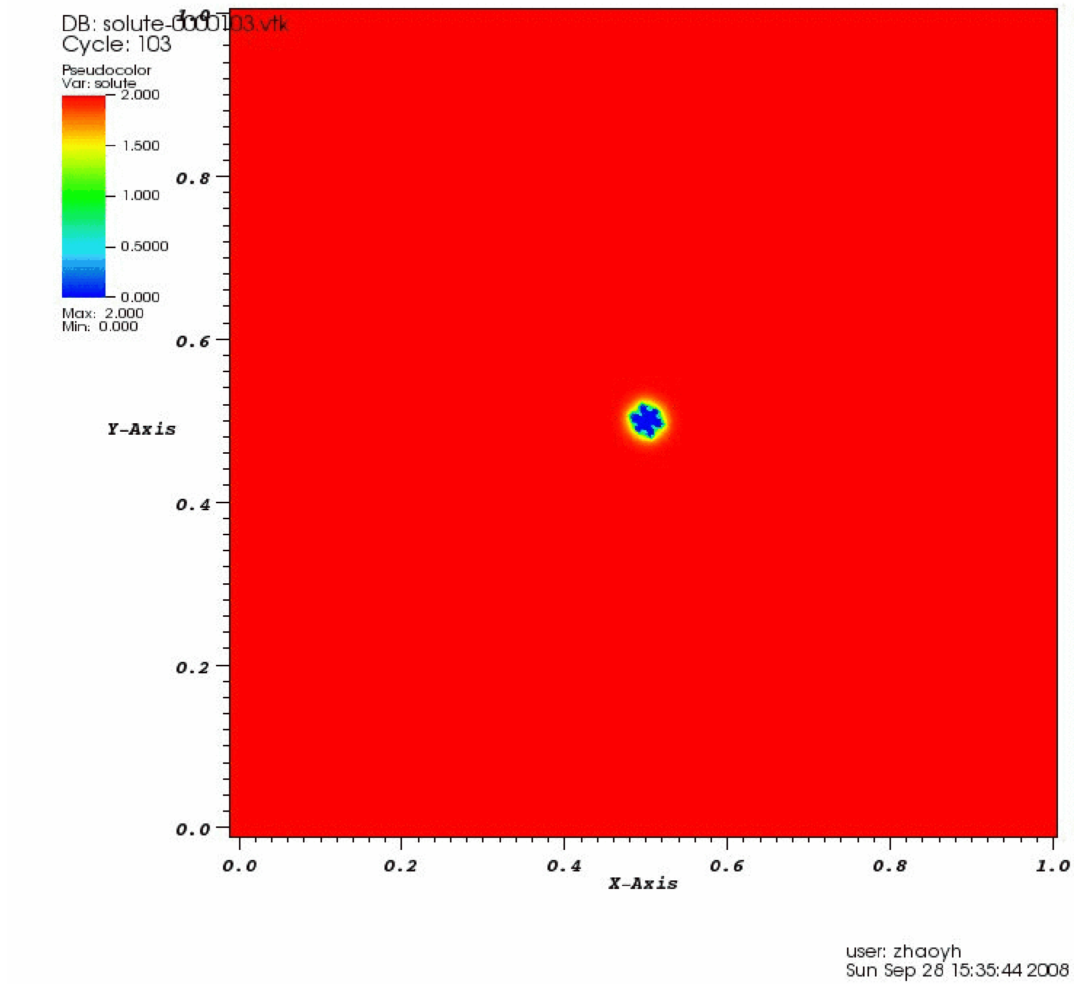

Three Dimensional Solute Precipitation

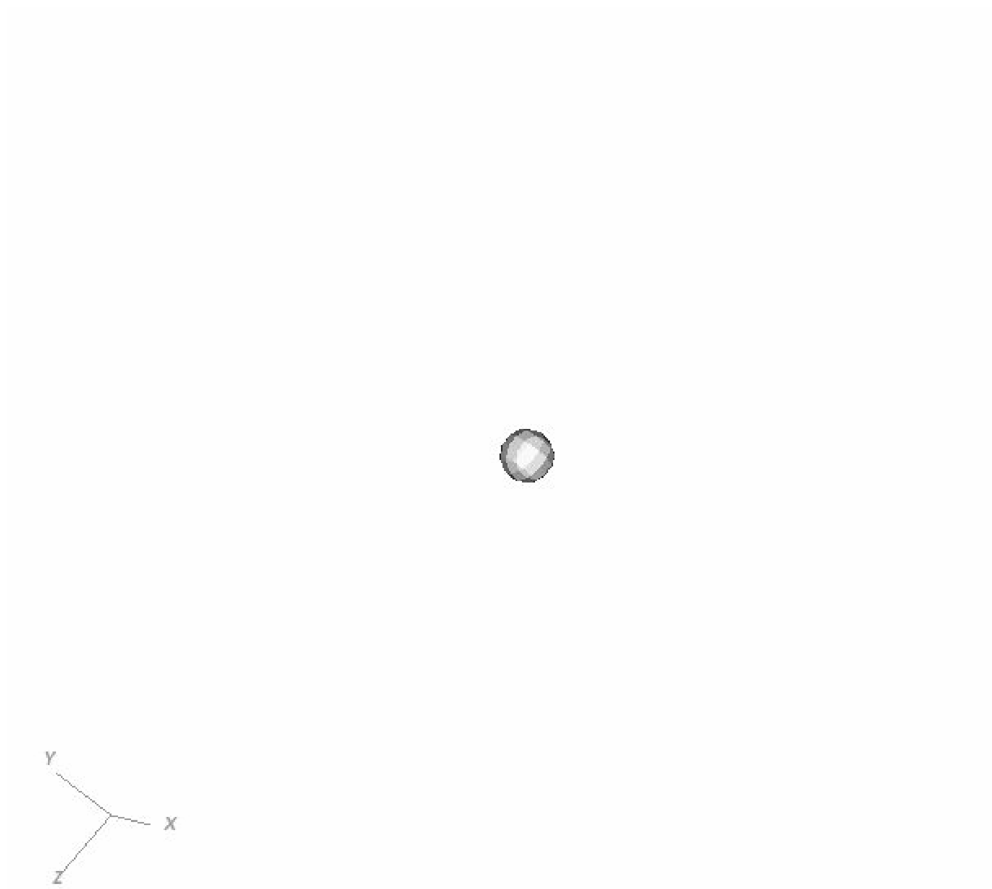

Dissolution is the opposite process of deposition

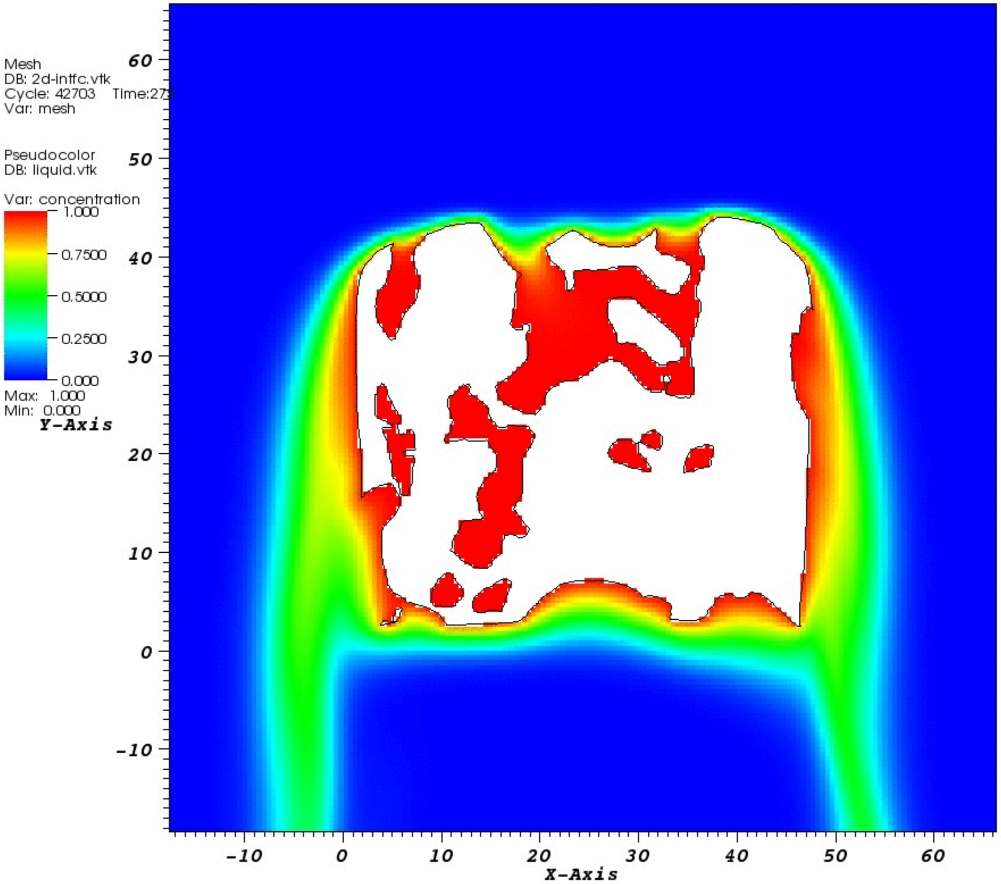

The Spring Model for two dimensional surface

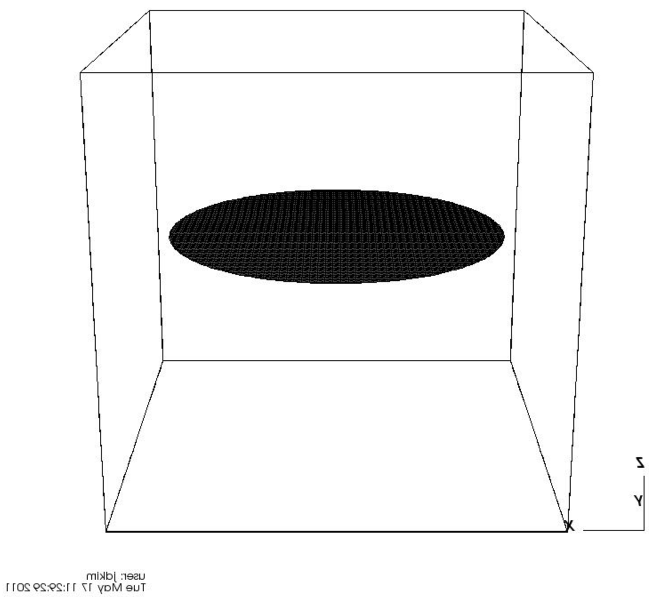

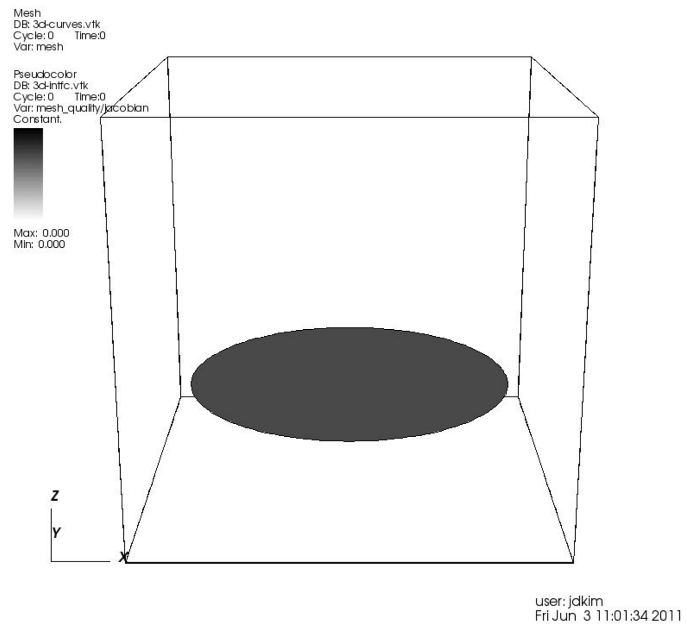

The X Parachute

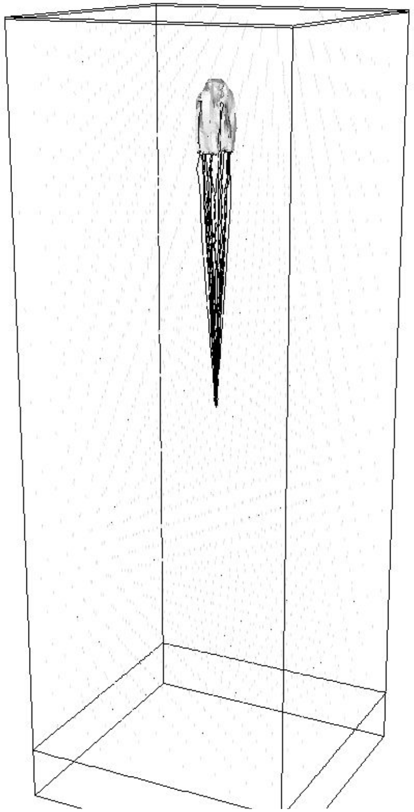

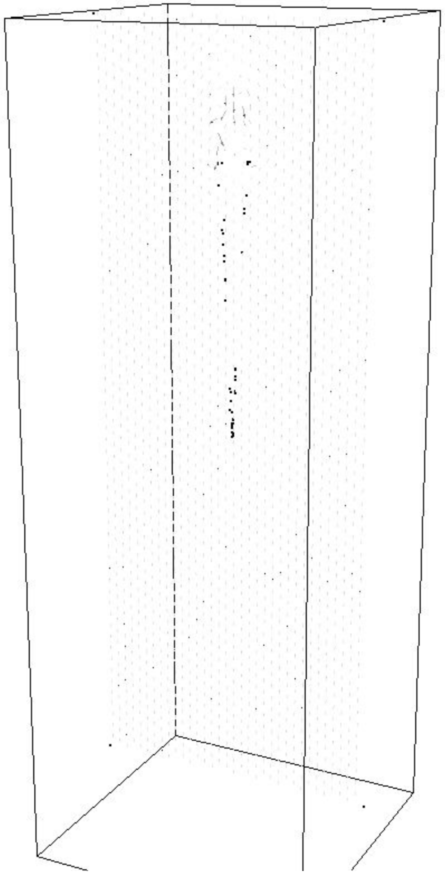

风力发电机的数值模拟

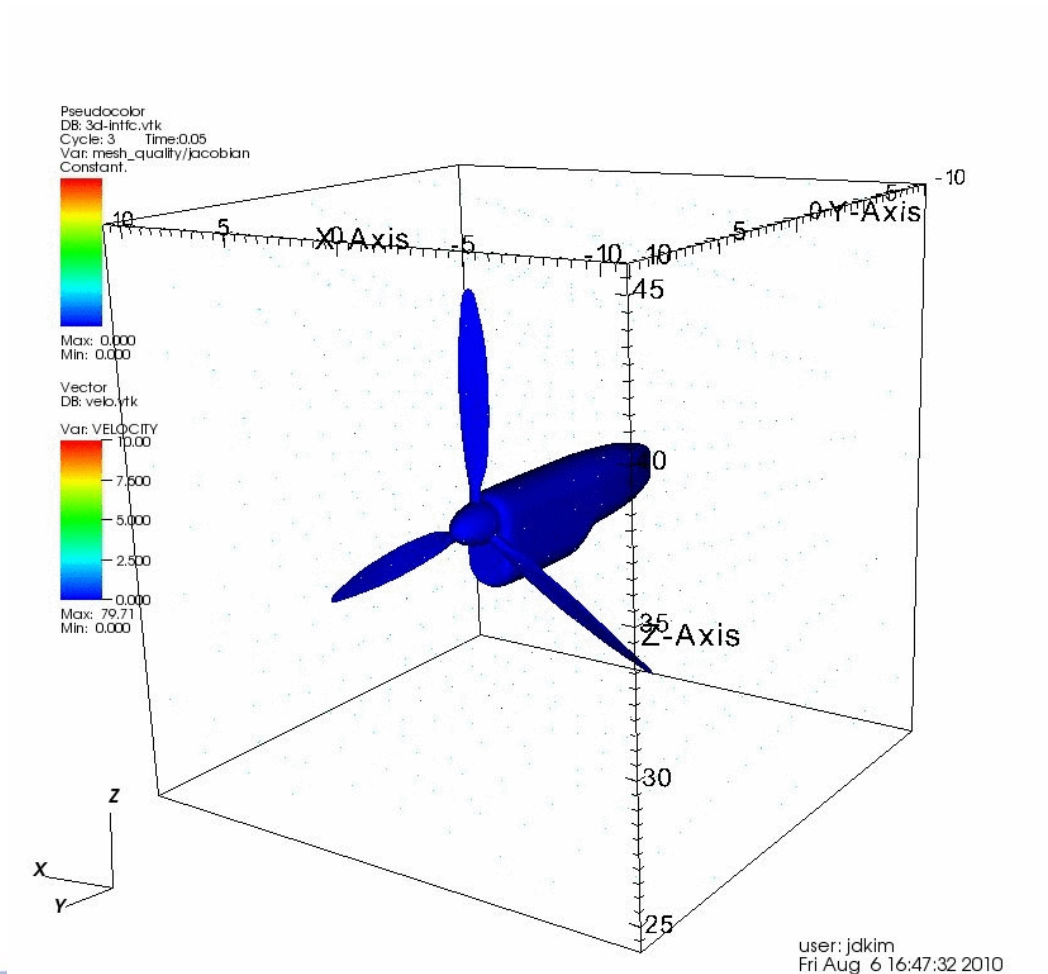
Pseudocolor
DB: 3d-intfc.vtk
Cycle: 3 Time:0.05
Var: mesh_quality/jacobian
Constant.
Max: 0.000
Min: 0.000
Vector
DB: velo.vtk
Var: VELOCITY
10.00
7.500
5.000
2.500
0.000
Max: 79.71
Min: 0.000
X-Axis
Y-Axis
Z-Axis
user: jdkim
Fri Aug 6 16:47:32 2010

Fluid-Rigid body interaction

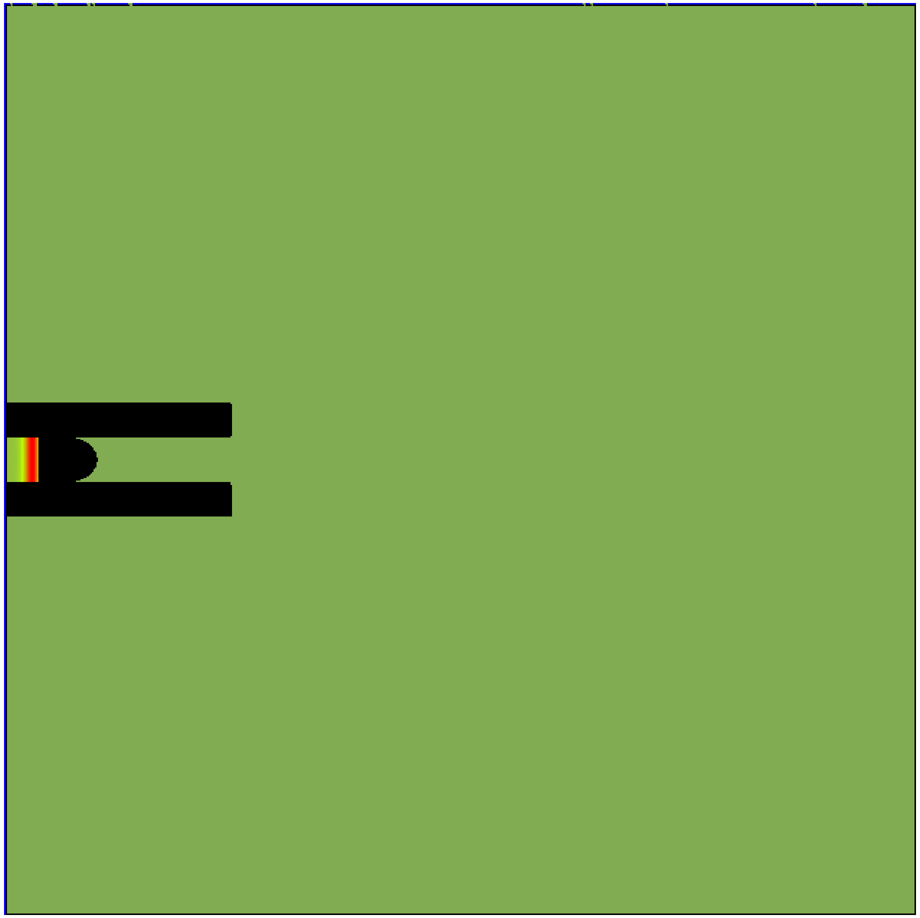

Scientific Discovery through Advanced Computing

Simulation of Cell Migration

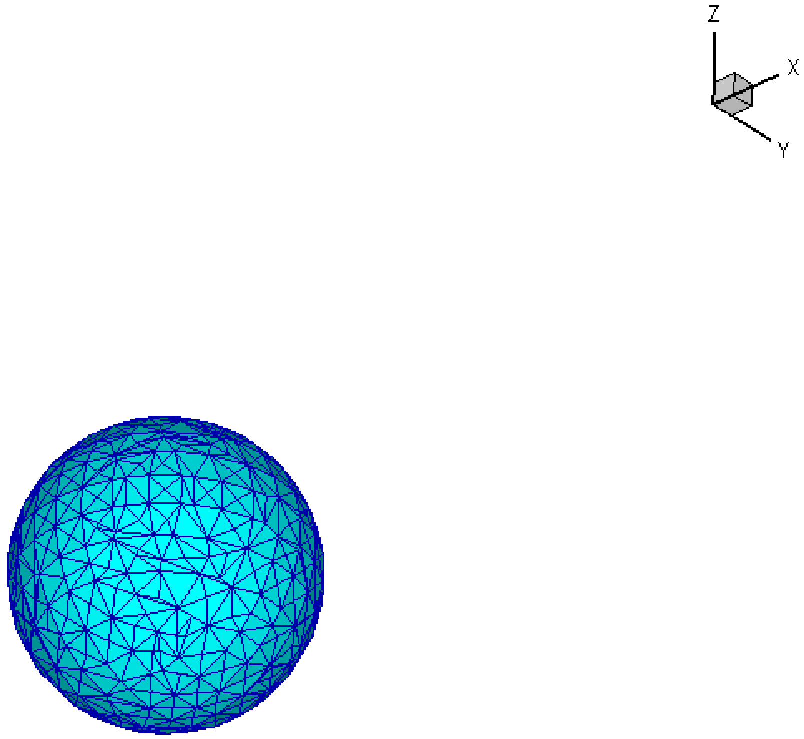

American and other exotic options

The Black-Schole Equation:

$$\frac{\partial C}{\partial \tau} - \gamma S \frac{\partial C}{\partial S} - \frac{1}{2}\sigma^2 S^2 \frac{\partial^2 C}{\partial^2 S} + (\gamma - D)C = 0,$$

$$\tau = T - t$$

Initial Condition:

$$C(S,0) = 0, \qquad S \le E$$

$$C(S,0) = S - E, \qquad S > E$$

The interface Condition at all time:

$$C_f = (S - E)$$

$$\frac{\partial C_f}{\partial S} = 1$$

American and many other exotic options are PDE free boundary problems. Front tracking provides an accurate tool to solve the basket hedging problems. We have already established 1-D and 2-D computational platform for such problems.

One Dimensional American options

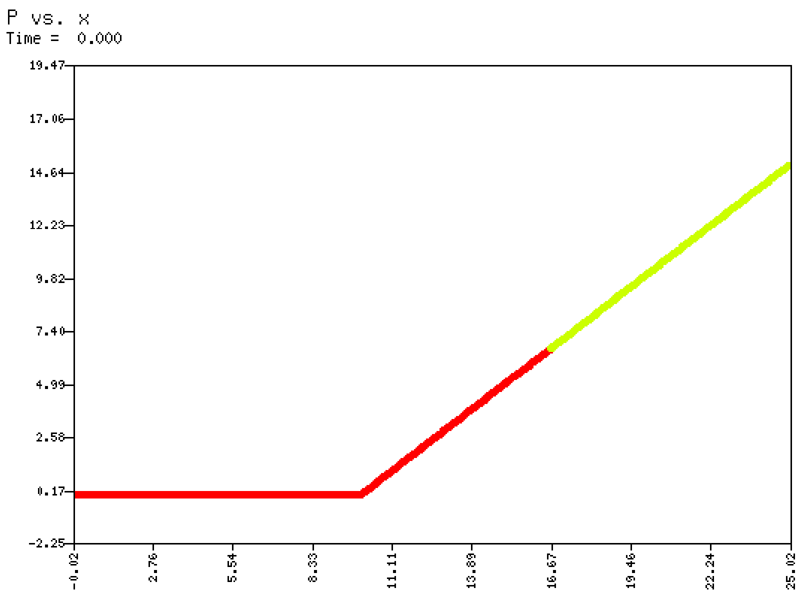

Front tracking on 1-D American call option

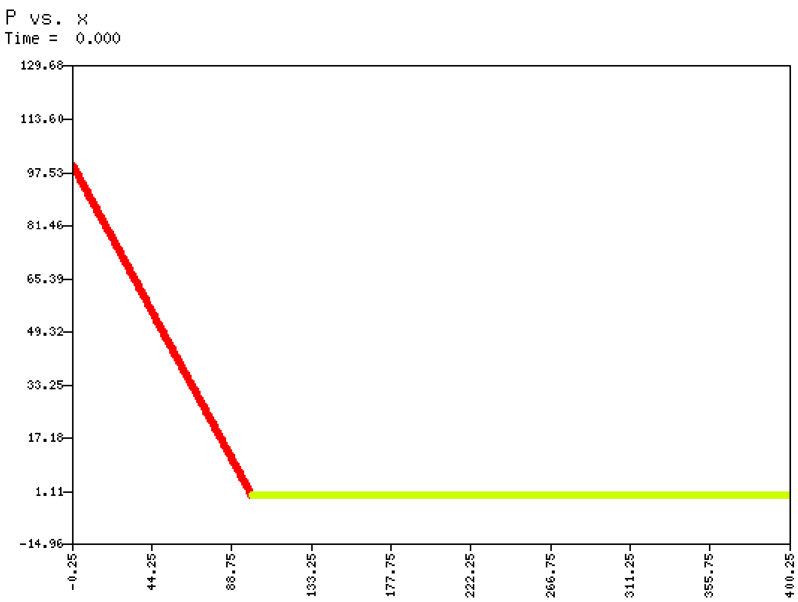

Front tracking on 1-D American put option

World's fastest computers (top 500)

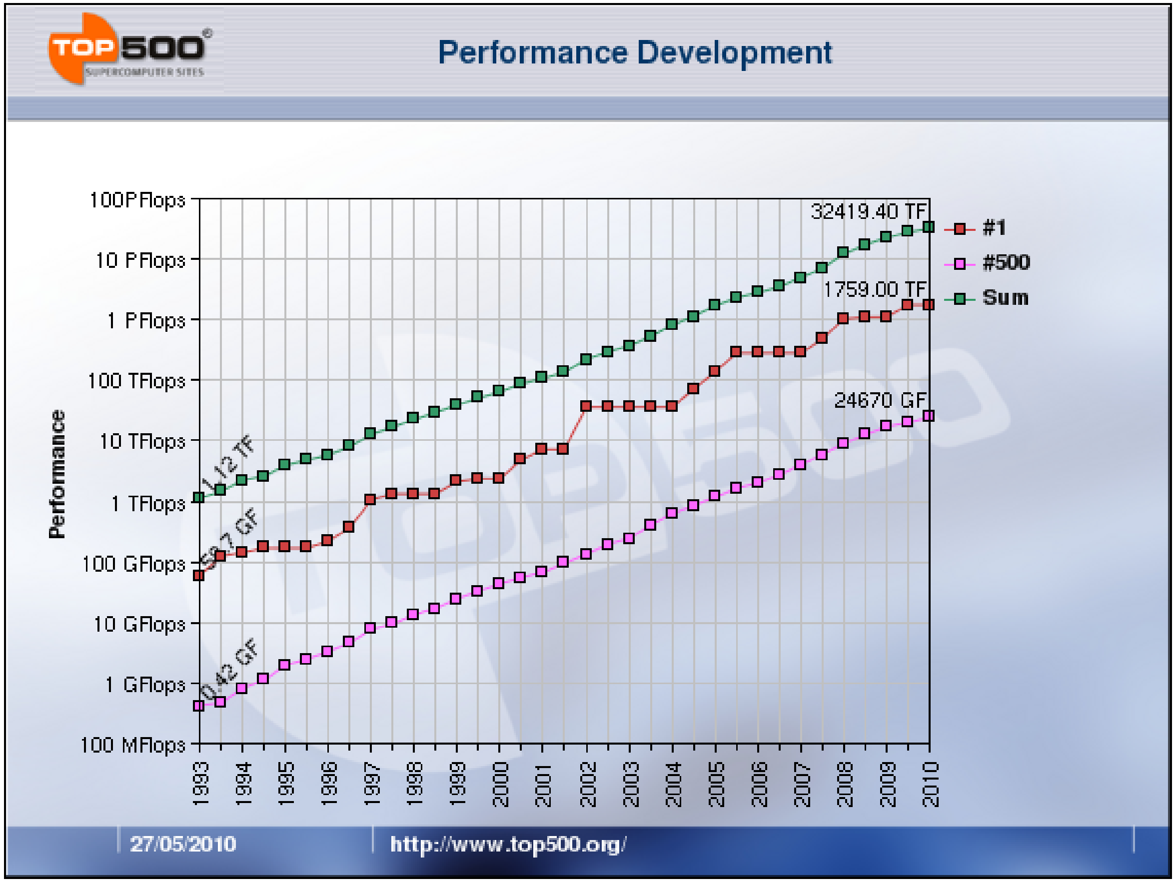

From mega scale, peta scale, to exa sacle

SciDAC
Scientific Discovery through Advanced Computing

Parallelization of Front Tracking

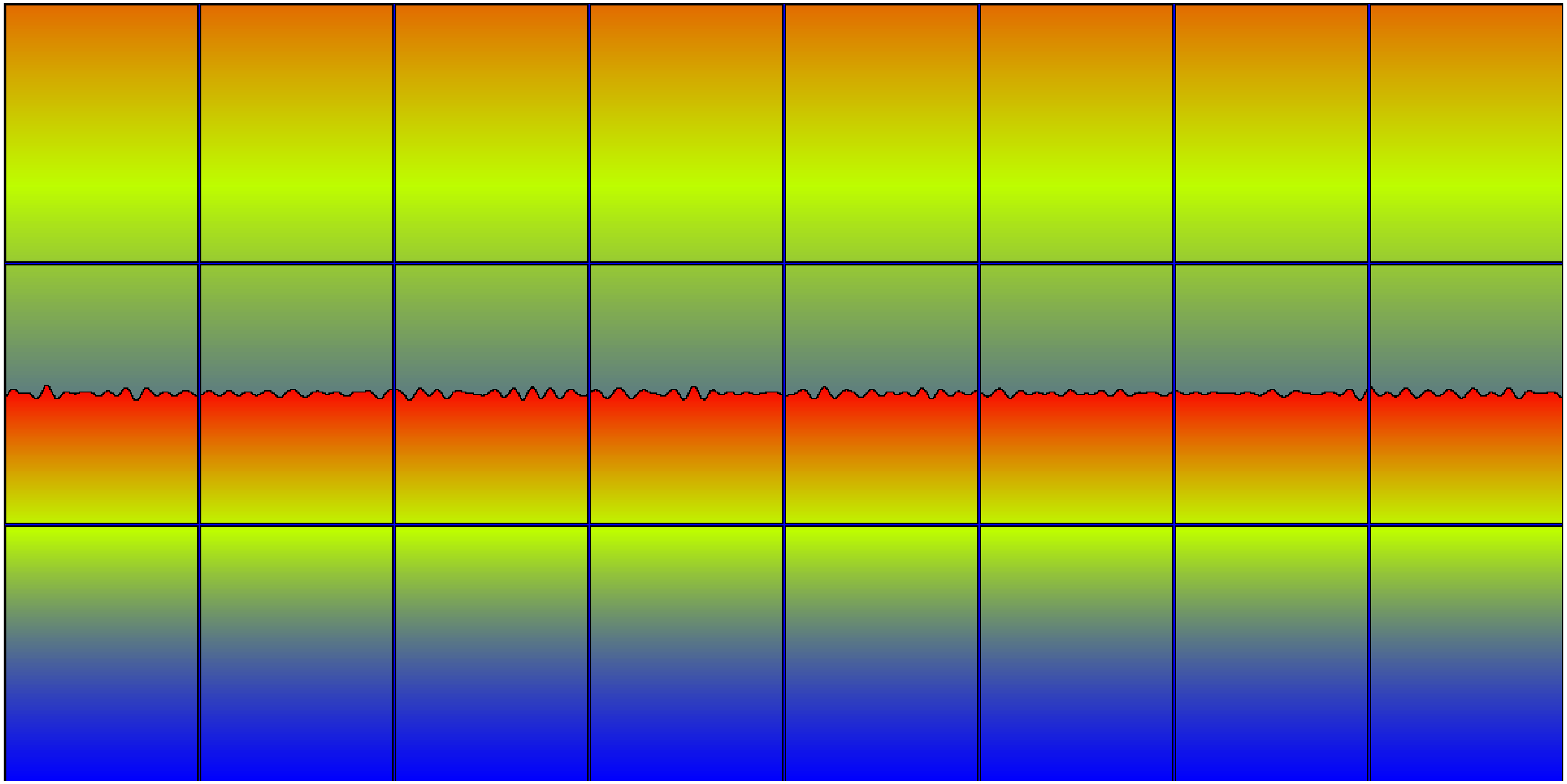

Parallel load balancing

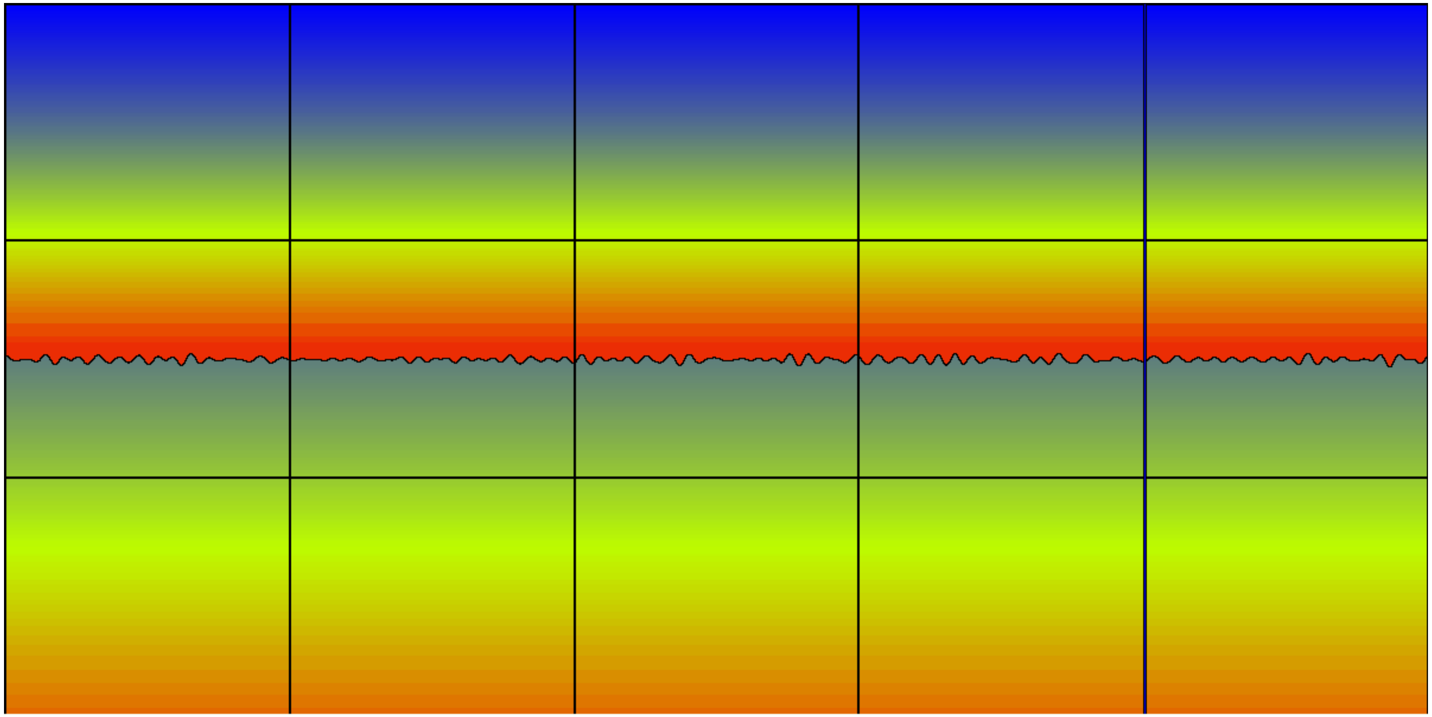

Like AMR, FronTier has encountered great obstacle in load balancing and parallel scaling. One important development is adaptive partition load balancing.Up to 8196 processors have been tested. No better for number larger than that.

Parallel Performance of FT

Performance of LGB

- Jet simulation
- 300-3million Triangles
- Bluegene/L 4096 cores

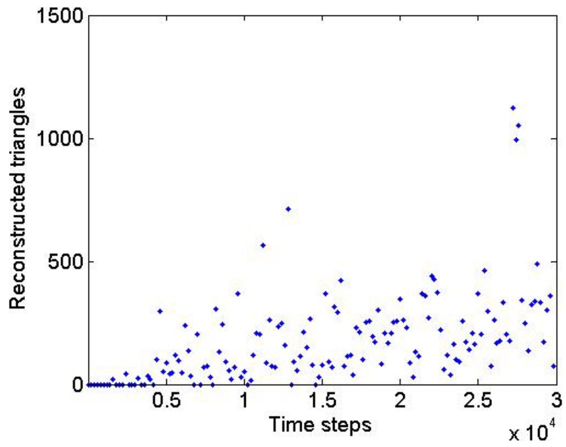

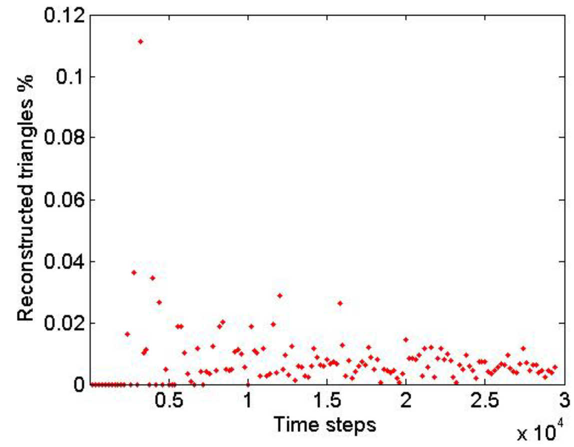

Weak scaling

- Rayleigh Instability
- Bluegene/L

Grid	Partition	nCores	Time to solution(s)	Ideal(s)
256×256×128	16×16×8	2048	157.1	157.1
256×256×256	16×16×16	4096	157.5	157.1
256×256×512	16×16×32	8192	158.2	157.1
256×256×1024	16×16×64	16384	159.8	157.1

A quotation from Albert Einstein

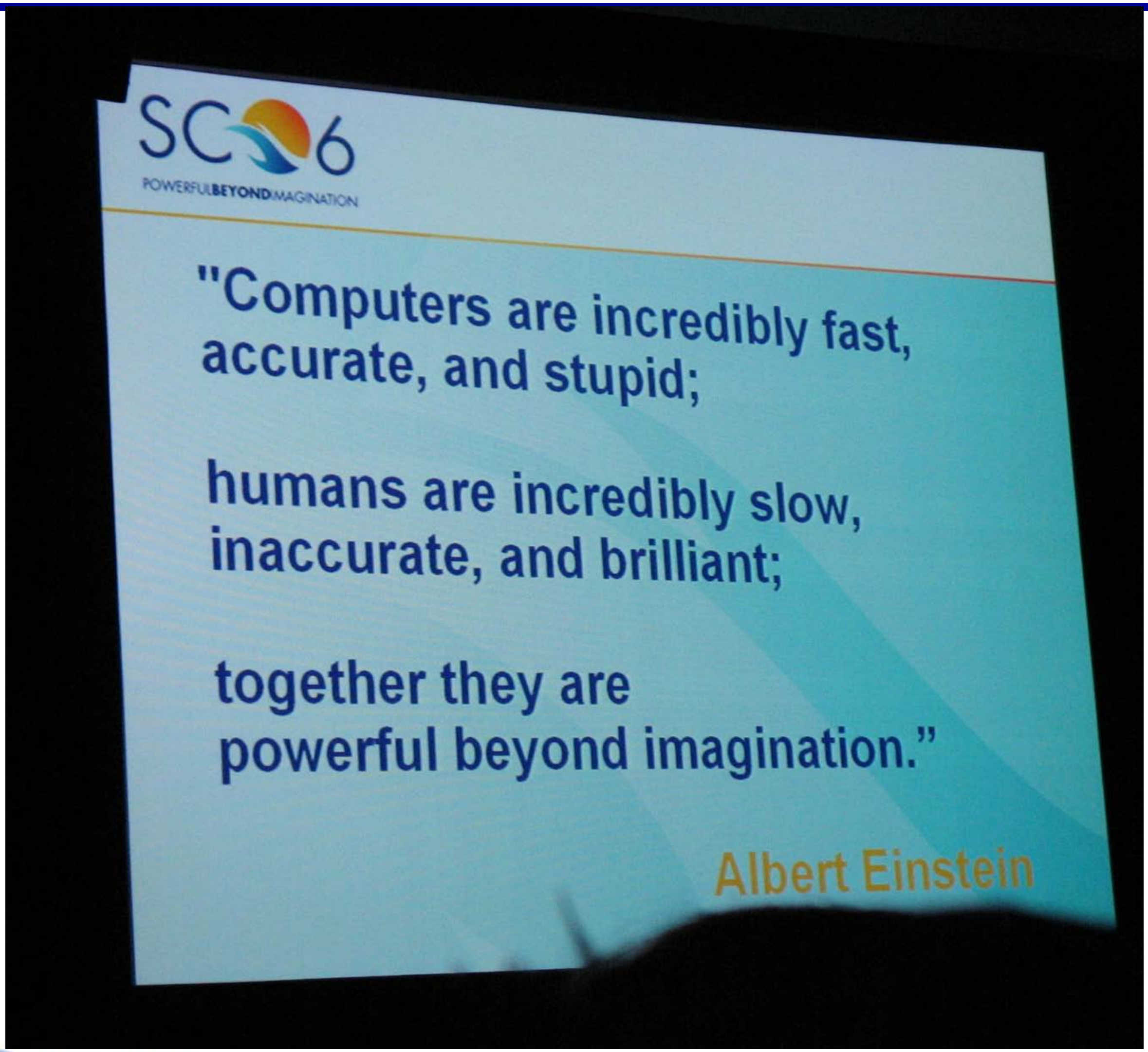

Major Computing Resources:

1. Stony Brook, AMS Department, galaxy cluster (over 500 processors)

2. Stony Brook, CEAS, Seawulf cluster

3. New York Blue: 103.22 teraflops

Thank you for your attention